



**Project title:** Radiation risk appraisal for detrimental effects from medical exposure during management of patients with lymphoma or brain tumour (SINFONIA)

**Grant Agreement:** 945196

**Call identifier:** NFRP-2019-2020

**Topic:** NFRP-2019-2020-14 Improving low-dose radiation risk appraisal in medicine

## **Deliverable D2.1 - Software tool on personalised dosimetry in radiological imaging and deep-learning guided algorithms**

<b>Lead partner:</b>	UoC (2)
<b>Author(s):</b>	John Stratakis, Marios Myronakis, John Damilakis
<b>Work Package:</b>	2
<b>Delivery as per Annex I:</b>	Month 36 (31.08.2023)
<b>Actual delivery:</b>	Month 36 (31.08.2023)
<b>Type:</b>	Report
<b>Dissemination level:</b>	Public

*“This project has received funding from the Euratom research and training programme 2019-2020 under grant agreement No 945196”*



## Table of Contents

List of figures .....	2
List of tables.....	3
Abbreviations.....	4
1. Development of methods to estimate patient organ dose from radiological examinations involved in cancer diagnosis, treatment, and follow-up .....	5
2. Data collection.....	5
3. Monte Carlo based dosimetric calculations: Software parametrization.....	6
4. Monte Carlo based dosimetric calculations: Simulations .....	8
5. Patient-specific 3D dose distributions.....	16
6. Delineation of radiosensitive organs within the primary exposed volume .....	17
7. Automatic CT couch/table removal.....	20
8. Dosimetric results.....	21
9. Software development – iDose web calculation tool.....	27
10. iDose web tool calculation interface .....	28
11. iDose Diagnostic X-ray Imaging Module – Computed Tomography.....	29
12. iDose Diagnostic X-ray Imaging Module – Digital Radiography .....	31
13. Automatic Imaged-Based Water-equivalent diameter (WED) calculation module .....	32
14. AI algorithm development – Rapid estimation of patient-specific organ doses from thoracic CT examinations using a deep learning network .....	35
15. AI algorithm development – Partially-irradiated liver dose estimation through a deep learning regression NN.....	41
16. AI algorithm development – Tube Current Modulation Reconstruction from Chest CT Images Using Deep-learning Regression Algorithms .....	49
17. iDoseAI organ dose prediction module – organ dose from CT thorax scans .....	54
18. iDoseAI organ dose prediction module – Partially-irradiated liver dose from CT thorax scans .....	56
19. iDoseAI organ dose prediction module – Tube Current Modulation Reconstruction.....	57
20. Dose and Risk report .....	59
21. References .....	61
22. Appendix - Hyperparameters Optimization Algorithms parametrization.....	63

## List of figures

Figure 1: The graphical user interface of ImpactMC. ....	7
Figure 2: ImpactMC project structure. ....	8
Figure 3: Graphical representation of extraction of longitudinally modulated tube current from DICOM header. Columns A and B represent z-axis position and tube current, respectively. ....	9
Figure 4: SpekCalc spectrum calculation software GUI. ....	10
Figure 5: A user defined spectrum and spectral data file. ....	11
Figure 6: Definition of the shaped filter material and density, angular increment, and thickness (Adapted from ImpactMC user-manual). ....	12
Figure 7: Simulation parameters of plain projection radiography with IMPACTMC - Distance focus center of rotation in correlation with focus to image receptor distance. ....	15
Figure 8: ImpactMC simulation of digital radiography (DR) AP irradiation, showing transverse, sagittal and coronal planes. ....	15
Figure 9: (a) CT image slices and (b) corresponding dose distribution in the thorax region. ....	16
Figure 10: Graphical representation of right lung contours overlaid on corresponding dose slices. ....	17
Figure 11: Automatic segmentation of bone structures using thresholding techniques. ....	18
Figure 12: Automatic segmentation of skin contour and lungs using thresholding techniques. ....	19
Figure 13: (a) original image slice of patient with pulmonary fibrosis; (b) image after morphological opening; (c) binarization – notice the couch has been already removed; (d) filling the empty space; (e) outline overlaid on original image. ....	20
Figure 14: UoC Medical Physics tools web site and login page of iDose organ dose estimation tool, which will be located at <a href="http://medphys-tools.uoc.gr">http://medphys-tools.uoc.gr</a> and <a href="http://idose.med.uoc.gr">idose.med.uoc.gr</a> . ....	27
Figure 15: iDose organ dose estimation tool initial toolbox page and selection of integrated personalized dosimetry tools. ....	28
Figure 16: iDose organ dose estimation tool navigation panels for hierarchical selection of dosimetry tools. ....	29
Figure 17: iDose web calculation tool interface accordion implementation overview. ....	30
Figure 18: iDose organ dose calculation tool - main calculation tab - adults. ....	30
Figure 19: iDose organ dose calculation tool - main calculation tab - adults. ....	31
Figure 20: Image-based WED tool inside iDose organ dose calculation tool with image upload capability. .	33
Figure 21: Image-based WED calculation from user-supplied DICOM series inside iDose organ calculation tool. ....	34
Figure 22: AI-based personalized organ dose estimation scheme without MC/segmentation implementation. ....	35
Figure 23: Personalized organ dose estimation scheme with MC/segmentation implementation for constructing ground truth data used in NN training. ....	36
Figure 24: DL-network architecture dependent and independent variables. ....	37
Figure 25: Plot of DL-predicted dose against Monte Carlo estimated dose for bone tissue. Linear regression is show with dashed line ( $R^2=0.826$ ). Perfect agreement is depicted with red line. ....	38
Figure 26: Plot of DL-predicted dose against Monte Carlo estimated dose for esophagus tissue. Linear regression is show with dashed line ( $R^2=0.877$ ). Perfect agreement is depicted with red line. ....	38
Figure 27: Plot of DL-predicted dose against Monte Carlo estimated dose for heart tissue. Linear regression is show with dashed line ( $R^2=0.877$ ). ....	39
Figure 28: Plot of DL- predicted dose against Monte Carlo estimated dose for lung tissue. Linear regression is show with dashed line ( $R^2=0.775$ ). Perfect agreement is depicted with red line. ....	39
Figure 29: Relative prediction error between deep-learning predicted and Monte Carlo estimated organ doses values in the test dataset (bones, oesophagus, heart, lung are depicted). ....	40
Figure 30: Schematic representation of a MC-based organ estimation methodology. ....	42

Figure 31: Missing CT abdomen data for MC-based organ calculation..... 42

Figure 32: Highly detailed whole-body anatomical family of XCAT digital phantoms. .... 43

Figure 33: Optimization strategy of a neural network architecture. .... 44

Figure 34: Hyperparameter tuning optimization algorithms. .... 45

Figure 35: Comparison of grid search and random search for minimizing a function with one important and one unimportant parameter (adapted from [17]). .... 46

Figure 36: Training model loss v/s Epochs graph. .... 48

Figure 37: Prediction on the train dataset based on the best model. .... 49

Figure 38: Prediction on the test dataset based on the best model. .... 49

Figure 39: Example of body segmentation in various consecutive slices using morphological operations.... 50

Figure 40: Differences in scan length, slice width and positioning of each patient reflect on WED values per slice. .... 51

Figure 41: Procedure to determine the normalized independent variable table. (Dependent variable not shown but included in the model). .... 51

Figure 42: General structure and flow of the deep-learning model (Dependent variable not shown but included in the model). .... 52

Figure 43: Validation loss and RMSE graph. .... 52

Figure 44: Relative difference between Actual and Predicted current modulation per patient. .... 53

Figure 45: Predicted versus real tube-current modulation values for various patients. .... 53

Figure 46: Predicted versus real tube-current modulation values overlaid on a coronal slice of the corresponding patient. .... 54

Figure 47: iDoseAI organ dose estimation tool navigation panels for of AI/ML thorax CT organ dose prediction module in accordion implementation overview..... 54

Figure 48: iDoseAI organ dose estimation tool navigation panels for of AI/ML thorax CT organ dose prediction module. .... 55

Figure 49: iDoseAI organ dose estimation tool navigation panels for AI/ML partially-irradiated organ prediction module (accordion implementation overview. .... 56

Figure 50: iDoseAI organ dose estimation tool navigation panels for AI/ML partially-irradiated organ (liver) prediction module. .... 56

Figure 51: iDoseAI organ dose estimation tool navigation panels for of AI/ML tube current modulation reconstruction prediction module. .... 58

Figure 52: iDose organ dose calculation tool - Dose and risk report calculation tab..... 59

Figure 53: iDose Dose and Risk Report example. .... 60

## List of tables

Table 1: Table 1: Scanner geometric parameters used to model the GE GSI Revolution 64 behavior. .... 8

Table 2: CT exposure settings and corresponding Monte Carlo parameters. .... 13

Table 3: CT exposure parameters for diagnostic CT scans. .... 13

Table 4: Exposure parameters for diagnostic radiology DR scans..... 14

Table 5: ImpactMC simulation/ exposure parameters for diagnostic radiology DR scans. .... 14

Table 6: Average error and standard deviation between deep learning network and Monte Carlo estimated organ-dose values..... 37

Table 7: Bayesian optimization vs Hyperband optimization algorithm properties..... 47

## Abbreviations

<b>3D</b>	Three-dimensional
<b>AP</b>	Anterior Posterior
<b>AI</b>	Artificial Intelligence
<b>ATCM</b>	Automatic Tube Current Modulation
<b>CT</b>	Computed Tomography
<b>CTDI</b>	Computed Tomography Dose Index
<b>DICOM</b>	Digital Imaging and Communication in Medicine
<b>DR</b>	Digital Radiography
<b>FTC</b>	Fixed Tube Current
<b>GPU</b>	Graphics Processing Unit
<b>GUI</b>	Graphical User Interface
<b>HTML</b>	HyperText Markup Language
<b>HU</b>	Hounsfield (scale) Unit
<b>kV</b>	kilovoltage
<b>LAT</b>	Lateral
<b>MC</b>	Monte Carlo
<b>ML</b>	Machine Learning
<b>NAS</b>	Network Attached Storage
<b>NURBS</b>	Non-uniform rational B-spline
<b>PA</b>	Posterior Anterior
<b>PACS</b>	Picture Archiving and Communications System
<b>RELU</b>	Rectified Linear Activation Functions
<b>SSDE</b>	Size specific Dose Estimate
<b>TCM</b>	Tube Current Modulation
<b>WED</b>	Water Equivalent Diameter
<b>XCAT</b>	extended Cardiac-Torso (XCAT) anatomical phantom

## 1. Development of methods to estimate patient organ dose from radiological examinations involved in cancer diagnosis, treatment, and follow-up

Lymphoma and brain tumor patients are representative examples of sensitive, extensive, and long-lasting followed up category of patients experiencing successive exposures in radiology, nuclear medicine, and radiation therapy. The longer post-exposure life expectancy of children and young adults increases the lifetime risks of developing radiation-induced malignancies. Furthermore, to assess stochastic radiogenic risks resulting from radiological examinations, the dose to specific radiosensitive organs should be estimated [1-4].

One of the objectives of the UoC-driven Tasks 2.1 and 2.3 was to propose methods for the accurate estimation of radiation dose to irradiated organ structures from radiological examinations associated with the diagnosis and radiotherapy treatment of benign and malignant tumors by considering patient size and exposure characteristics with the use of patient-specific computational models.

The proposed methods for scanner-specific and patient-specific organ-dose estimation, is based on procedures that combine Monte Carlo (MC) computational techniques and patient computed tomography (CT) scans. In general, the procedure is composed of five steps, detailed in subsequent paragraphs; (a) collection of suitable patient CT exams; (b) extraction of examinations' parameters; (c) MC dosimetric computations; (d) three-dimensional (3D) patient-specific dose distribution output and (e) correlation between dose and patient characteristics.

Three-dimensional dose distributions were used as input data to (a) automatically extract organ doses ; (b) estimate doses for partially exposed organs and organs exposed to scattered radiation through modelling of additional patient volume, not included in the initial CT-based patient-models; (c) estimate organ doses rapidly and accurately during or immediately after a radiological examination through modelling of the relationship between patient-specific characteristics and dose-response.

## 2. Data collection

Examinations from 226 pediatric and 308 adult lymphoma and brain tumor patients were included in this task. In addition, exposure data from 570 conventional x-ray examinations were retrieved. All images and exposure were selected and extracted from the local Picture Archiving and Communication System (PACS) database following specific data protection guidelines as proposed by the SINFONIA Data Management Board to ensure data privacy and security.

### **Data Privacy and Security**

Data was collected on-site, using a local secure network through PACS Digital Imaging and Communication in Medicine (DICOM) protocol. Before delineation and MC simulations, all CT images collected were anonymized and patient and exams id were kept in a different password protected archive, so as images' identifiers were all limited to alphanumeric characters with no direct connection to patient personal data.

### **Anonymization**

Proper handling is essential for maintaining patient privacy when dealing with sensitive patient data. [5]. There are mainly two methods to de-identify patient-related information through a DICOM header strategy [6]. The first method is anonymization which removes information carried by header elements or replaces the information with random data such that the remaining information cannot be used to reveal the

patient identity at all. Another method, pseudo-anonymization, is implemented by replacing these fields using artificial identifiers that could be used to track down the real identity of the patient in case of clinical analysis. An in-house developed application was used to access and pseudo-anonymize DICOM Metadata.

### 3. Monte Carlo based dosimetric calculations: Software parametrization

#### **Monte Carlo software for dosimetric computations**

The MC software selected for dosimetric computations was ImpactMC (version 1.6, CT Imaging© GMBH, Erlangen, Germany). ImpactMC is a software package providing fast calculation of 3D dose distributions for CT scans using MC algorithms [7-9].

Based on volumetric data as input, an individualized voxelized MC simulation is performed to calculate the dose deposited. Dose is calculated on a per image voxel basis, considering all available physical interactions. ImpactMC's output comprises of parametric dose images in which every voxel carries the normalized dose (to Computed Tomography Dose Index- CTDI) of the initial image grid.

The generated 3D dose distributions are useful to estimate organ doses and to calculate effective dose of individual scans. Figure 1 demonstrates the graphical user interface (GUI). The GUI consists of two main panels - one for parameter input and one for visualization. At the bottom of the image viewer a panel gives information on dose, density and material for the voxel selected with the mouse cursor.

ImpactMC utilizes any available Nvidia graphics processing unit (GPU) to accelerate computations. In conjunction with high-speed parallel processing within the GPU, higher GPU memory bandwidth facilitates greater compute efficiency compared to CPU-only intensive calculations.

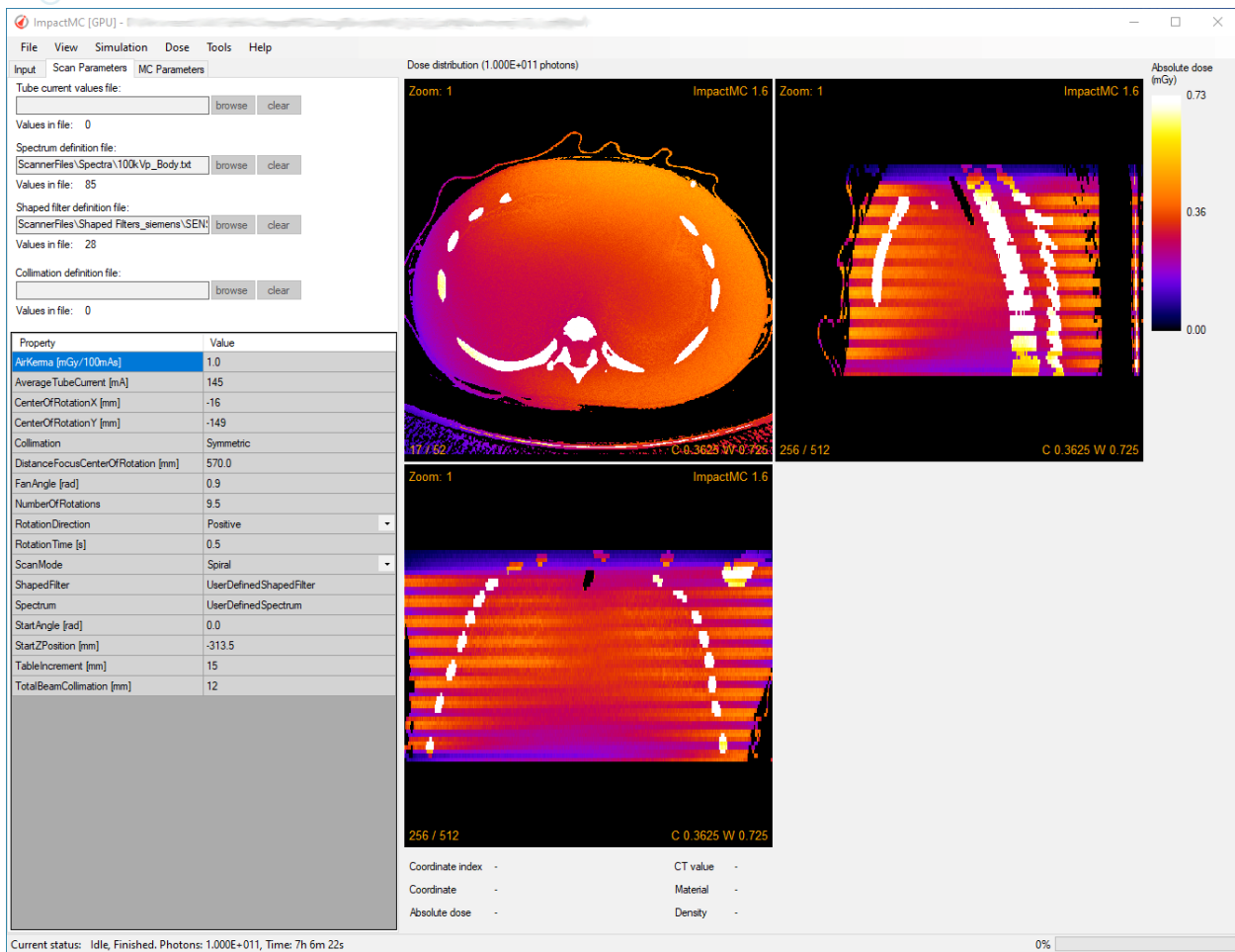


Figure 1: The graphical user interface of ImpactMC.

Each estimation of the dose distribution in a CT volume starts with setting up an ImpactMC project.

Figure 2 provides an overview of the project structure. The following input data were required by the software to start the dose computation procedure:

1. Input volume: The input volume represents the scanned patient or phantom; a set of CT reconstructed images from one examination, in DICOM format.
2. Scan parameters: Data for beam spectrum, filtration, and geometrical specifications
3. Simulation parameters: The number of x-rays depositing energy in the input volume was selected.



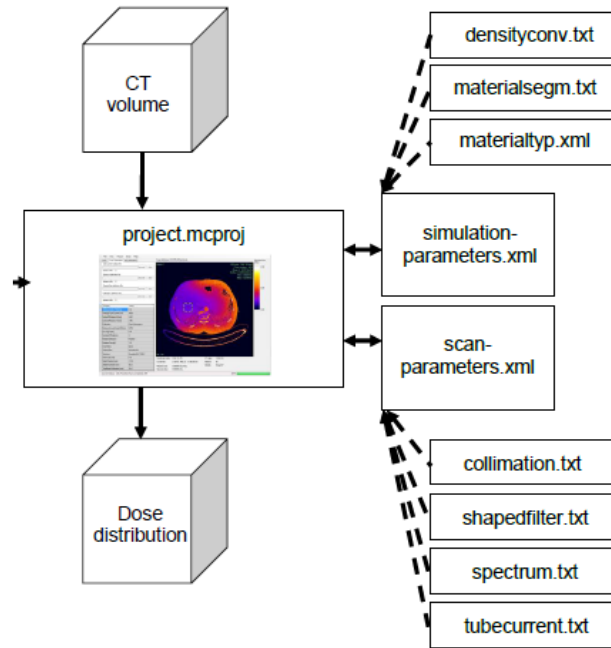


Figure 2: ImpactMC project structure.

## 4. Monte Carlo based dosimetric calculations: Simulations

### Diagnostic CT scans simulations

Scanner-specific dose computations required the parameterization of the MC software according to operating and physical characteristics of each CT scanner [10]. The scanner model simulated was based on the scanner used in our institution (GE GSI Revolution 64). Data for x-ray beam spectra, beam shaping devices (bow-tie filters) and geometrical specifications were provided by the manufacturer (Table 1) and converted to input parameters suitable for the Monte Carlo software.

Focus to Isocenter (mm)	Fan Angle (deg)	Beam collimation (mm)	Beam shaping devices
539	58	20.0	Small, Medium, Large

Table 1: Table 1: Scanner geometric parameters used to model the GE GSI Revolution 64 behavior.

### Simulation of CT Scanner tube current modulation

The DICOM header of each reconstructed image (z) included a unique mAz value along with the corresponding table location. Each mAz value is the average of the angularly and longitudinally modulated values applied over the gantry rotation used to reconstruct this z-th image. mAz profile values were retrieved from the DICOM header of the image data using ImageJ manipulation software and used as a custom tube current file for the MC simulation software (Figure 3).

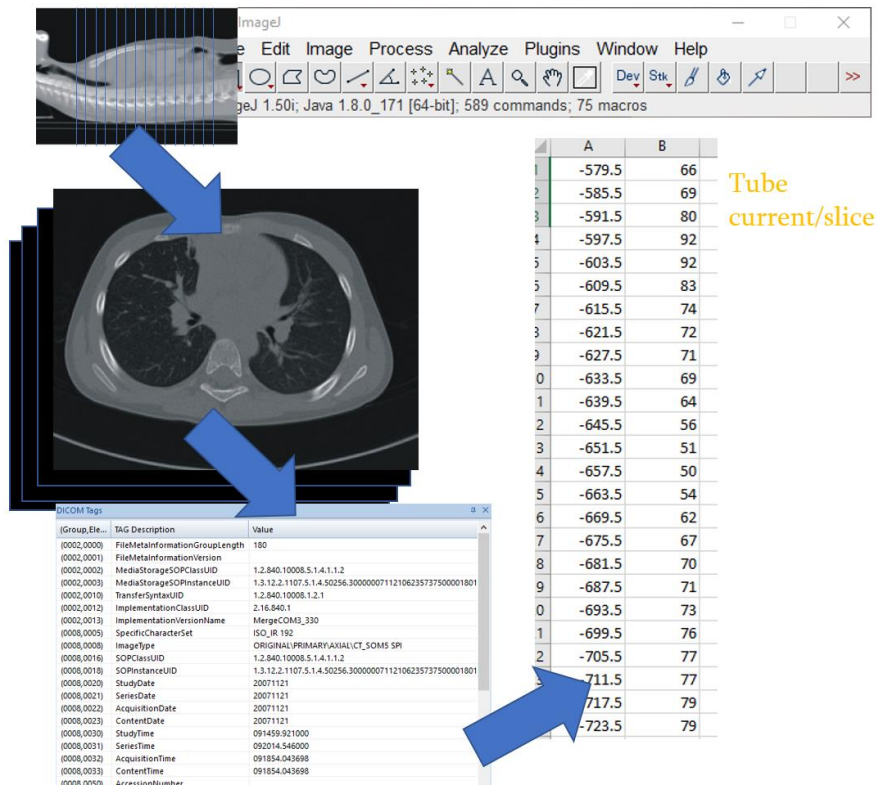


Figure 3: Graphical representation of extraction of longitudinally modulated tube current from DICOM header. Columns A and B represent z-axis position and tube current, respectively.

### Determination of scanner parameters – Spectral characteristics

Beam spectra for various modes of operation, were produced for each modality using SpekCalc spectrum calculation program [11]. SpekCalc allows the user to calculate and display the x-ray spectra emitted from tungsten-anode x-ray tubes. The underlying theoretical description for the bremsstrahlung and characteristic x-ray production was taken from a recently published model [12]. The user can select tube potential in kVp, the take-off angle and the amount of filtration. The resulting spectrum can be calculated, displayed, and saved/exported for later use. Beam quality parameters such as the half-value-layer, in mm of aluminum and copper, and the mean beam energy, in keV, can also be considered as depicted in Figure 4. Filtration can be selected in mm, for 7 materials (eg, Al, Co, Zn, etc).

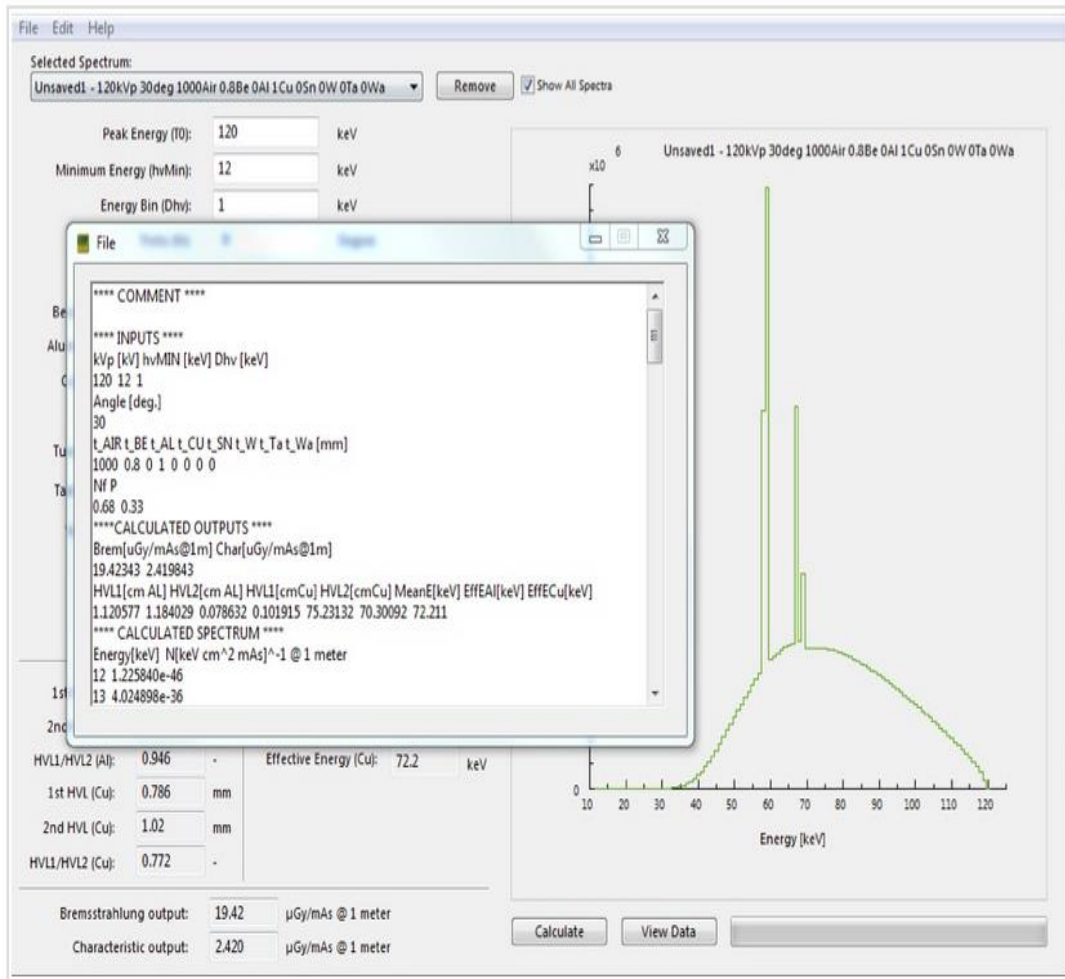
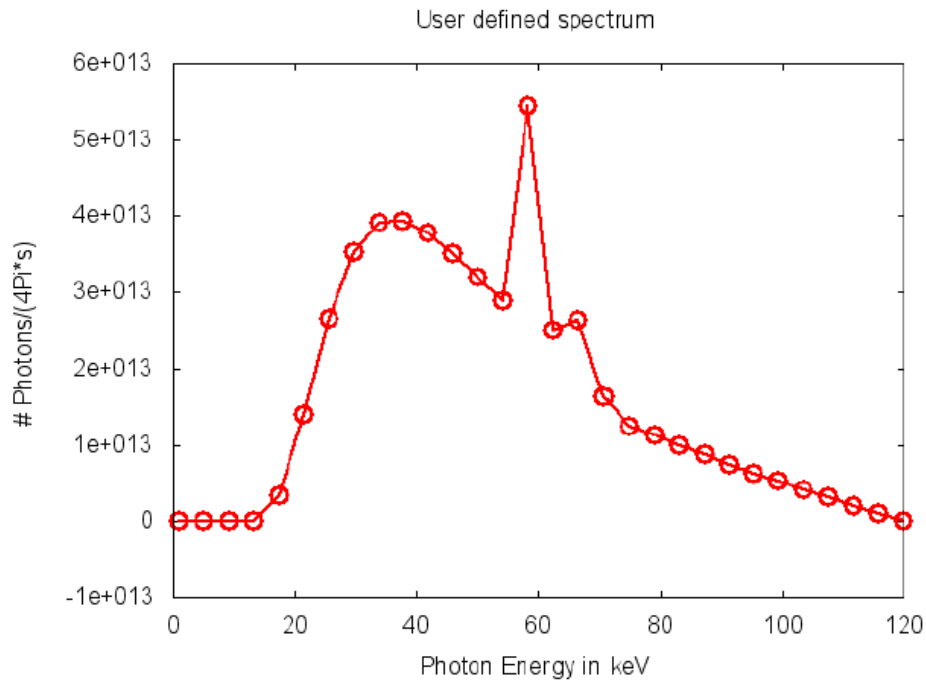


Figure 4: SpekCalc spectrum calculation software GUI.

The structure of IMPACTMC 's spectrum text file consists of several entries, each defining the number of photons at a certain energy level (Figure 5: A user defined spectrum and spectral data file.). Each line has the following syntax:

energy e (in keV), number of photons in the spectrum in energy bin e

The values for e must be positive, monotonically increasing, and equidistant. The number of photons did not have to be normalized because normalization was done by the software, if necessary. This text file was imported using the GUI.



```
# Spectral Data File
# Energy, Photons/(4Pi*s)
1.000, 0.0
5.103, 9.1194e-030
9.207, 1.7386e+006
13.310, 9.3135e+010
17.414, 3.3558e+012
21.517, 1.3956e+013
25.621, 2.6502e+013
29.724, 3.5191e+013
33.828, 3.9030e+013
```

Figure 5: A user defined spectrum and spectral data file.

**Determination of scanner parameters – CT shaping filters modelling**

In ImpactMC software, the user has the option to include a shaped filter where the thickness of the filter is varying with the fan angle at the x-ray source in the MC simulations. The shaped filter can be switched off and on from the GUI (Figure 6). The user can add a shaped filter from a specification file. In this case the values for filter material and thickness are read from the file according to the following file structure:

- line 1: Filter (keyword)
- line 2: # Name of the material (mandatory comment line)
- line 3: Name of the material, e.g. Al. (software specific name)
- line 4: # Density of the material (g/cm^3) (mandatory comment line)
- line 5: Density of the material in g per cm3,
- line 6: # Angular increment (°) (mandatory comment line)
- line 7: Angular increment between the given thickness values in degrees.

line 8: # Thickness array (mm) (mandatory comment line)

line 9: thickness of the shaped filter at angle = 0°, i.e. in the middle of the fan beam

line 10: thickness of the shaped filter at angle +/- angular increment

following lines: thickness of the shaped filter at n angle +/- angular increment

```

Filter
# Name of the material
Al
# Density of the material (g/cm^3)
2.7
# Angular increment (°)
5.0
# Thickness array (mm)
0.49014
0.74040
1.30470
2.15470
3.26210
4.89555

Filter
# Name of the material
C
# Density of the material (g/cm^3)
1.88
# Angular increment (°)
10.0
# Thickness array (mm)
0.49014
0.74040
1.30470
2.15470

```

Figure 6: Definition of the shaped filter material and density, angular increment, and thickness (Adapted from ImpactMC user-manual).

**Diagnostic CT scans protocols**

CT exposure for pediatric and adult cases were performed with predefined protocols suitable for specific anatomic site-imaging in all scanners. These protocols have specific settings that were translated to corresponding parameter values in the Monte Carlo software. For each voxelized model, the number of rotations per simulation was calculated based on the length of the imaged volume, beam collimation and pitch. Table 2 contains a list of CT settings and their equivalent value in the Monte Carlo software. CT exposure parameters for diagnostic CT scans are tabulated in Table 2.

CT Setting	Monte Carlo Parameter
kV	User defined file with spectrum
Beam Collimation (mm)	Total Beam Collimation (mm)
mA modulation	Tube Current Values File
mA fixed	Average Tube Current
Pitch	Table Feed (*)
Rotation time (s)	Rotation Time (s)

Table 2: CT exposure settings and corresponding Monte Carlo parameters.

(\*) Pitch is converted to table feed using the total beam collimation and pitch value

For diagnostic CT, the following protocols were simulated:

Patient Population	Anatomical Site	kV	mAs	Acquisition Type	Filter Type	Collimation (mm)	Pitch
Adult	Head	120	Modulated	Axial	Medium	20	1
Adult	Head	120	Modulated	Helical	Medium	20	0.531
Adult	Thorax	120	Modulated	Helical	Large	20	0.968
Adult	Abdomen/ Pelvis	120	Modulated	Helical	Large	40	0.984
Pediatric	Head	80	Modulated	Helical	Medium	20	0.968
Pediatric	Thorax	80	Modulated	Helical	Medium	20	0.968
Pediatric	Abdomen/Pelvis	120	Modulated	Helical	Medium	20	0.968

Table 3: CT exposure parameters for diagnostic CT scans.

### Digital Radiography examinations simulations

Simulating plain digital radiography requires similar spectral and protocol parameters with CT. However, several geometric alterations must be implemented to MC software to simulate plain radiography projection. A reference point, which relates to MC parameter “CenterOfRotation”, needs to be provided, and subsequently distance from x-ray focus is supplied along with in-plane fan angle of the x-ray beam, number of rotations (1 for plain radiography), scan mode (localizer for plain radiography), projection angle and z-position of the x-ray tube, and collimation of x-ray beam in z-direction. Modelled protocols are depicted in Table 4. Exposure parameters are depicted in Table 5.

Patient Population	Anatomical Site	kV	mAs	Views
Adult	Head	80	AEC	AP, PA, Lat
Adult	Thorax	120	AEC	AP, PA, Lat
Adult	Abdomen	75-90	AEC	AP, PA, Lat
Pediatric	Head	70	AEC	AP, PA, Lat
Pediatric	Thorax	120	AEC	AP, PA, Lat
Pediatric	Abdomen	75-90	AEC	AP, PA, Lat

Table 4: Exposure parameters for diagnostic radiology DR scans.

Parameter	Value
Air Kerma	1.12 mGy/ 100 mAs
Average tube current	400 mA
Number of rotations	1
Rotation time	0.02 s
Scan mode	Localizer
Start angle	0 (AP)
Table increment	0

Table 5: ImpactMC simulation/ exposure parameters for diagnostic radiology DR scans.

(\*) The mAs value was determined per patient. To streamline the simulation procedure, we normalized to an average value along the patients and then scaled back to obtain the absolute value. (\*\*) AP, PA, Lat: Anterior-Posterior, Posterior-Anterior, and Lateral views respectively.

Radiography simulations were performed in lateral (LAT), Posterior-Anterior (PA) and Anterior-Posterior (AP) position. Figures 7 and 8 illustrate MC simulations of plain radiography projections in terms of project parametrization and resulting distributions shown in terms of body anatomical planes.



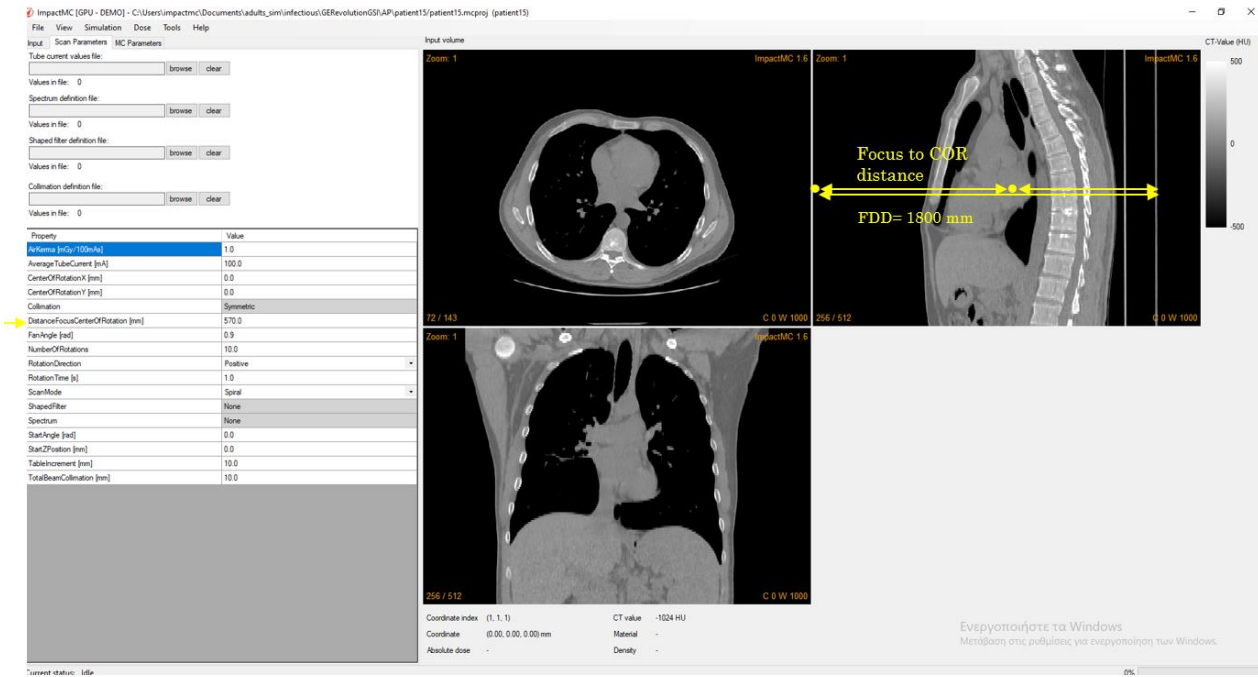


Figure 7: Simulation parameters of plain projection radiography with IMPACTMC - Distance focus center of rotation in correlation with focus to image receptor distance.

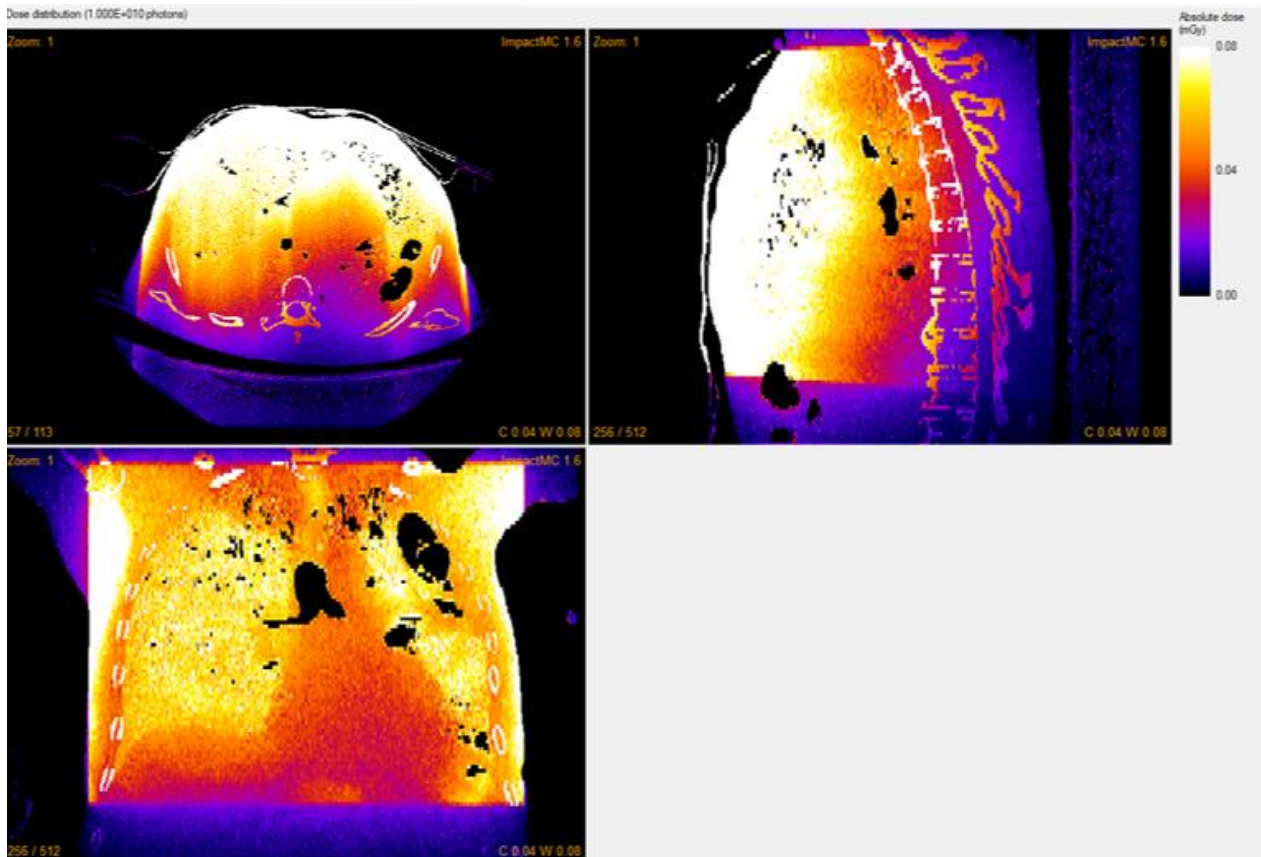


Figure 8: ImpactMC simulation of digital radiography (DR) AP irradiation, showing transverse, sagittal and coronal planes.



## 5. Patient-specific 3D dose distributions

The MC software output after each computation is in the form of a 3D dose distribution (Figures 9 a, b), based on the physical properties (i.e., attenuation, composition, and size) obtained from the patient-specific input. Each slice in the dose volume corresponds to the same slice of patient-input. Each pixel in a specific slice of the input volume has a corresponding dose value in the 3D dose distribution output. The dose distribution was exported in DICOM file format. The unit of dose values in the 3D volume was mGy/mGy per 100mAs. Organ dose information was extracted from 3D dose distributions through appropriate delineation.

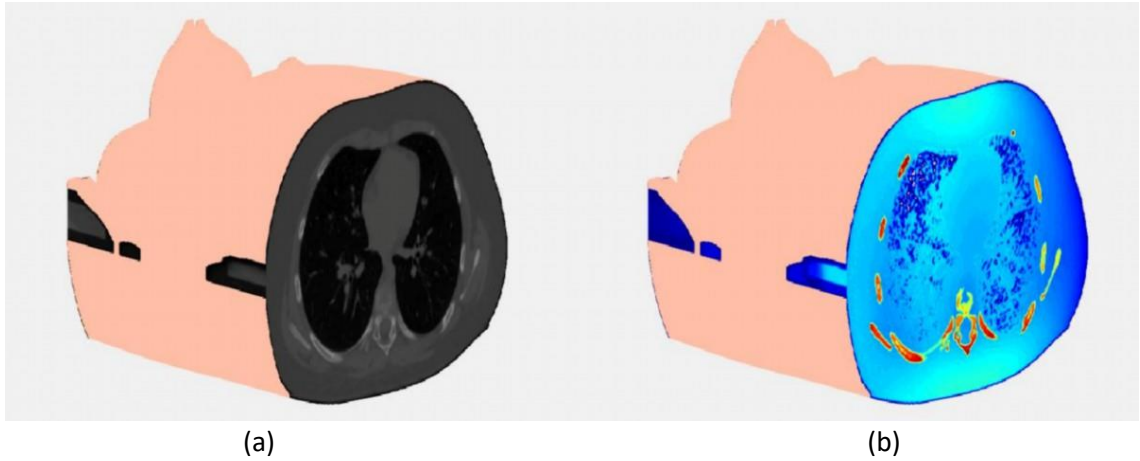


Figure 9: (a) CT image slices and (b) corresponding dose distribution in the thorax region.

The contours of an organ were overlaid on the corresponding slices of the dose distribution (Figure 10) and the respective dose was extracted. The dose over the whole organ was computed as:

$$D = \sum_i^N D_i \quad (1)$$

where,  $D_i$  is the dose within the contour at slice  $i$ , and  $N$  the total number of slices that contain contours of a specific organ. The calculated dose ( $D$ ) was normalized to 100 mA, pitch factor ( $p$ ) equal to one, and rotation time ( $t_{rot}$ ) equal to one second using the following formula:

$$D_n = D \times \frac{p \times 100}{t_{rot} \times mA} \quad (2)$$

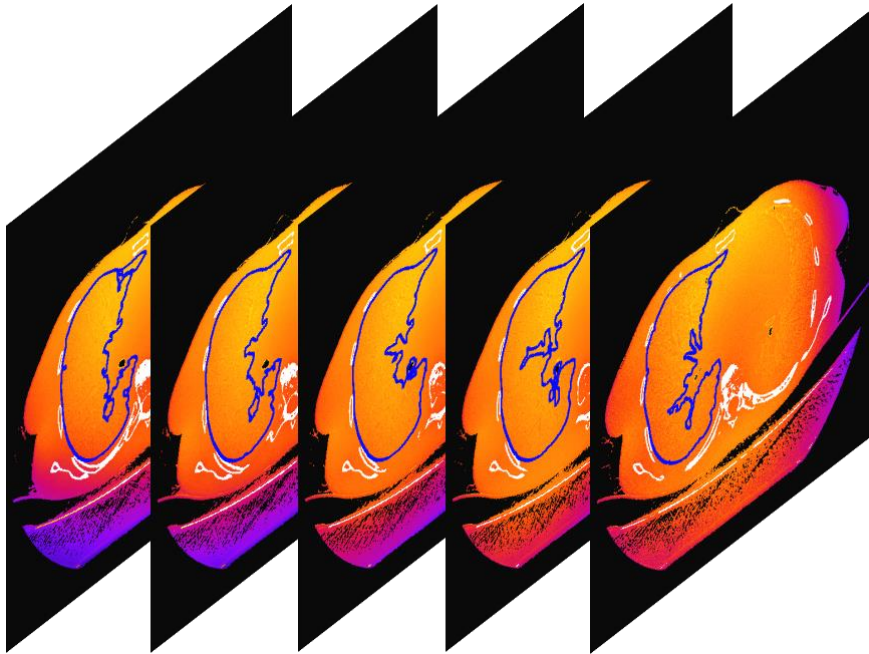


Figure 10: Graphical representation of right lung contours overlaid on corresponding dose slices.

Due to the large number of simulated results, organ dose calculation procedure was automated. Relevant in-house algorithms were implemented to provide unsupervised organ dose calculation, WED values and corresponding linear regression outcomes.

## 6. Delineation of radiosensitive organs within the primary exposed volume

Open-source tools were utilized to delineate radiosensitive organs within the primary exposed volume of all pediatric and adult CT scans. Structures that were automatically delineated were bones, lungs, and the outline of the patient. To segment these structures, thresholding techniques were utilized [13-14]. Lung entities were manually selected after thresholding, and bone structures were automatically assembled using the analyze particles ImageJ tool, which extracts and measures objects in binary or thresholded images. Size and circularity of the structures were altered accordingly to efficiently trace the contours (Figure 12 and Figure 12).

Esophagus, breast, heart, bladder, kidneys, liver, gallbladder, pancreas, stomach, and spleen were manually delineated by a radiologist using a Wacom tablet for added accuracy and by adjusting the brightness and contrast of the image to optimum levels.



Figure 11: Automatic segmentation of bone structures using thresholding techniques.

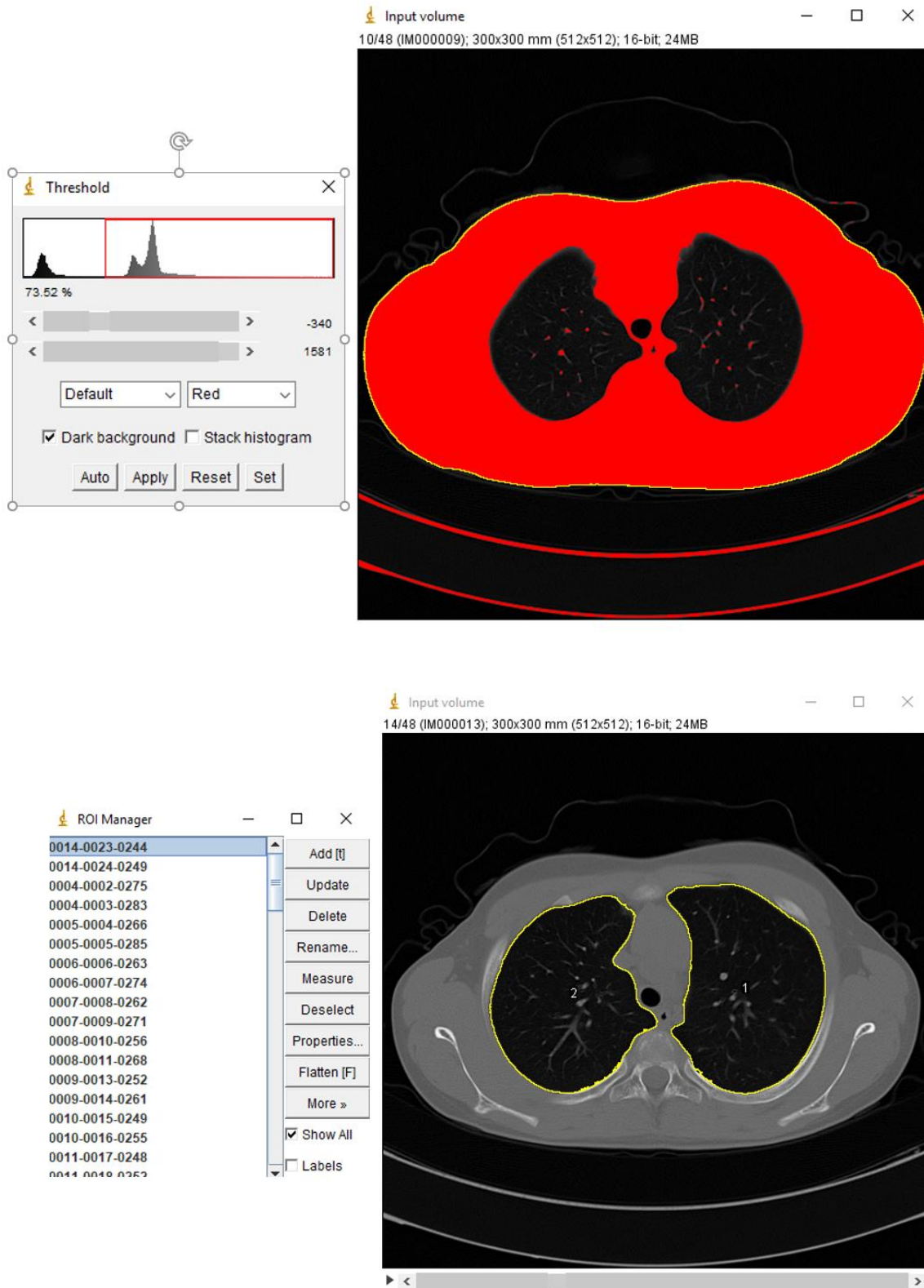


Figure 12: Automatic segmentation of skin contour and lungs using thresholding techniques.

## 7. Automatic CT couch/table removal

Accurate patient skin segmentation requires detailed delineation of the patient body outline on the CT slice without including the CT couch/table. In radiation therapy, body, organ and tissue delineation is part of the treatment planning routine, hence, body outline is readily available. In diagnostic radiology, such delineations are not usually provided.

Within the scope of this project, an algorithm to automatically delineate the patient body and remove the couch from each CT slice was developed (body segmentation). The algorithm is based on morphological operations applied on each image slice (Fig. 13 a). A square structuring element with heuristically determined size equal to 12 pixels was used to perform morphological opening. This step effectively removed small structures in the vicinity of the body and preserved the body shape and size (Fig. 13 b). The next step was conversion of the image to binary using Otsu's method to determine the single HU threshold between background and any other structure. During this step, the couch is usually removed from the image without affecting the body size or shape (Fig. 13 c).

In addition, since lungs and other low-density tissues are likely to produce empty space (holes) in the binarized image within the region defined by the body shape, this empty space was filled by detection of zero value locations that were not connected with the image borders (Fig. 13 d). In the final step, non-zero areas that were not connected were identified and the largest area was kept (i.e. the body) as seen in Fig. 13e.

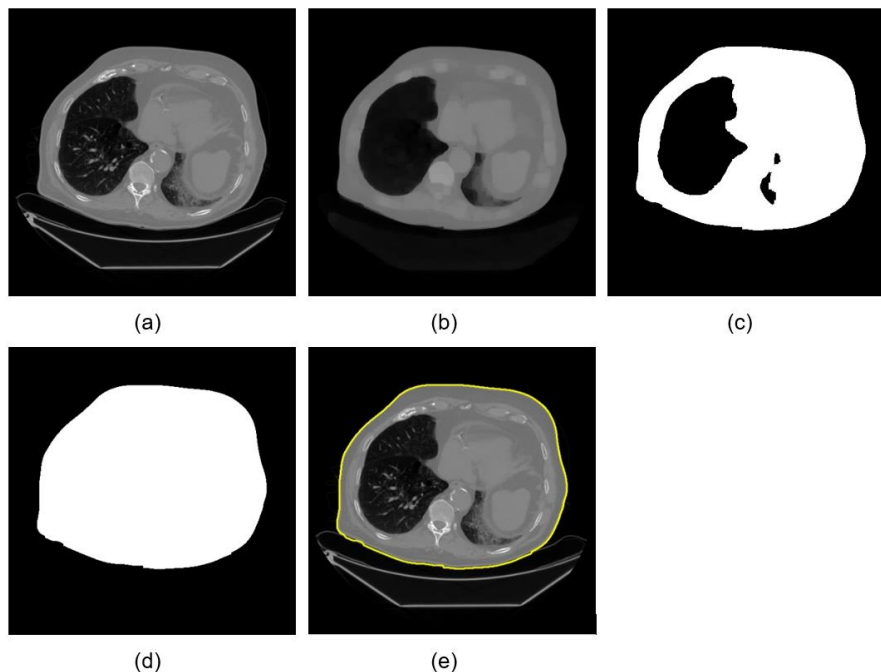


Figure 13: (a) original image slice of patient with pulmonary fibrosis; (b) image after morphological opening; (c) binarization – notice the couch has been already removed; (d) filling the empty space; (e) outline overlaid on original image.

## 8. Dosimetric results

### Correlation of organ doses to Water Equivalent Diameter (WED)

Water Equivalent Diameter (WED) and organ dose correlation was determined through univariate regression analysis. The estimated regression function was of the exponential form:

$$y = a \cdot e^{b \cdot x} \quad (2)$$

were the independent variable,  $x$ , corresponds to the WED value in millimeter (mm) units, estimated per patient as described previously. The WED was measured at the central axial plane crossing the geometrical center of the heart. The variable  $y$ , corresponds to the dependent variable, organ dose in mGy/mGy/100mAs (or similar normalized unit). Parameters  $a$  and  $b$  were estimated for each patient-specific WED at each organ dose computed by the MC software. The coefficient of determination  $R^2$ , was used as a measure to assess the strength of correlation between WED and organ dose.

In the following sections Tables are demonstrated with the results of regression analysis for all WED and organ dose correlations. Furthermore, representative graphs for exponential fits depicting WED and organ dose correlations are provided. Parameters appearing on the tables are explicated as follows:

Organ: The name of the organ (bone, breast, esophagus, heart, lungs, etc)

Scanner: The name of the simulated scanner (GE: GE Revolution GSI 64)

Region: Anatomical Region (Head, Thorax, Abdomen/Pelvis)

kV: The kV beam setting of the computed dose data

AEC: True (1) if TCM was used or False (0) if tube current was fixed (applicable in CT)

$a, b$ : Fit parameters of  $y = ae^{bx}$



**Organ dose conversion coefficients: Parametric fits for Diagnostic CT X-ray Imaging – Adult Patients**

Region	Scanner	kV	AEC	Organ	a	b
Head	GE	120	1	bones	0.03205	-5.628E-03
Head	GE	120	1	brain	0.01391	-5.079E-03
Head	GE	120	1	eye	0.04783	-9.390E-03
Head	GE	120	1	oralmucosa	0.02688	-7.500E-03
Head	GE	120	1	salivaryglands	0.01486	-4.090E-03

Region	Scanner	kV	AEC	Organ	a	b
Thorax	GE	120	1	lungs	0.02223	-6.432E-03
Thorax	GE	120	1	heart	0.01643	-5.060E-03
Thorax	GE	120	1	bone	0.02644	-5.454E-03
Thorax	GE	120	1	esophagus	0.01995	-6.425E-03
Thorax	GE	120	1	skin	0.01027	-4.034E-03
Thorax	GE	120	1	breast	0.008752	-0.006347

Region	Scanner	kV	AEC	Organ	a	b
Abdomen	GE	120	1	adrenals	0.01691	-5.4510E-03
Abdomen	GE	120	1	gallbladder	0.01951	-5.2020E-03
Abdomen	GE	120	1	kidneys	0.02190	-5.7730E-03
Abdomen	GE	120	1	liver	0.01761	-5.1640E-03
Abdomen	GE	120	1	pancreas	0.02012	-5.6270E-03
Abdomen	GE	120	1	spleen	0.01749	-5.0000E-03

**Organ dose conversion coefficients: Parametric fits for Diagnostic CT X-ray Imaging – Pediatric Patients**

Region	Scanner	kV	AEC	Organ	a	b
Head	GE	120	1	Bones	0.05616	-0.01062
Head	GE	120	1	Brain	0.0151	-0.007148
Head	GE	120	1	Eye bulbs	0.01185	-0.005608
Head	GE	120	1	Eye lens	0.01175	-0.005566
Head	GE	120	1	Oral mucosa	0.1045	-0.02218
Head	GE	120	1	Salivary glands	0.05178	-0.01625

Region	Scanner	kV	AEC	Organ	a	b
Thorax	GE	120	1	lungs	0.01107	-0.004676
Thorax	GE	120	1	heart	0.0118	-0.004392
Thorax	GE	120	1	bone	0.02801	-0.006054
Thorax	GE	120	1	esophagus	0.009993	-0.003954
Thorax	GE	120	1	skin	0.009268	-0.004666

Region	Scanner	kV	AEC	Organ	a	b
Abdomen	GE	120	1	Bone	0.15	-0.01484
Abdomen	GE	120	1	Bladder	0.07857	-0.01488
Abdomen	GE	120	1	Kidney	0.02273	-0.007905
Abdomen	GE	120	1	Liver	0.02467	-0.009895
Abdomen	GE	120	1	Rectum	0.01591	-0.007117
Abdomen	GE	120	1	Spleen	0.02047	-0.008127
Abdomen	GE	120	1	Stomach	0.009906	-0.003883



**Organ dose conversion coefficients: Parametric fits for Diagnostic DR Planar X-ray Imaging – Adult Patients**

Region	Scanner	kV	Organ	a	b
Head PA	DR	70	bone	0.01514	-1.7360E-03
Head PA	DR	70	brain	0.02760	-7.5070E-03
Head PA	DR	70	eye_bulbs	0.03336	-1.4030E-03
Head PA	DR	70	eye_lens	0.02765	-7.3570E-04
Head PA	DR	70	oral_mucosa	0.04486	-5.8430E-03
Head PA	DR	70	skin	0.03594	-1.1240E-02

Region	Scanner	kV	Organ	a	b
Thorax PA	DR	120	bones	0.04740	-4.9990E-03
Thorax PA	DR	120	breast	0.01683	-7.8890E-03
Thorax PA	DR	120	esophagus	0.00901	-3.2010E-03
Thorax PA	DR	120	heart	0.00747	-3.7060E-03
Thorax PA	DR	120	lungs	0.01830	-4.4740E-03

Region	Scanner	kV	Organ	a	b
Thorax LLAT	DR	120	bones	0.02443	-4.7000E-03
Thorax LLAT	DR	120	breast	0.03267	-6.1310E-03
Thorax LLAT	DR	120	heart	0.01720	-5.8220E-03
Thorax LLAT	DR	120	lungs	0.01164	-3.4930E-03

Region	Scanner	kV	Organ	a	b
Thorax AP	DR	120	bones	0.03474	-6.0070E-03
Thorax AP	DR	120	breast	0.03325	-4.1970E-03
Thorax AP	DR	120	esophagus	0.02202	-6.5210E-03
Thorax AP	DR	120	heart	0.02470	-4.6640E-03
Thorax AP	DR	120	lungs	0.02123	-4.7950E-03

Region	Scanner	kV	Organ	a	b
Abdomen AP	DR	75	adrenals	0.02698	-1.0020E-02
Abdomen AP	DR	75	esophagus	0.04808	-1.2390E-02
Abdomen AP	DR	75	kidneys	0.04364	-1.1720E-02

Abdomen AP	DR	75	liver	0.03516	-7.8230E-03
Abdomen AP	DR	75	pancreas	0.04611	-8.7280E-03
Abdomen AP	DR	75	spleen	0.10740	-1.5800E-02
Abdomen AP	DR	75	stomach	0.03870	-7.3660E-03

Region	Scanner	kV	Organ	a	b
Abdomen PA	DR	75	adrenals	0.01860	-7.0030E-03
Abdomen PA	DR	75	esophagus	0.00431	-4.3450E-03
Abdomen PA	DR	75	kidneys	0.03743	-7.6020E-03
Abdomen PA	DR	75	liver	0.00130	-6.9450E-03
Abdomen PA	DR	75	pancreas	0.00803	-6.5070E-03
Abdomen PA	DR	75	spleen	0.01322	-4.2470E-03
Abdomen PA	DR	75	stomach	0.01837	-9.4330E-03

Region	Scanner	kV	Organ	a	b
Abdomen RLAT	DR	80	adrenals	0.02380	-8.9430E-03
Abdomen RLAT	DR	80	esophagus	0.17320	-1.6340E-02
Abdomen RLAT	DR	80	kidneys	0.02755	-7.4000E-03
Abdomen RLAT	DR	80	liver	0.15430	-1.9180E-02
Abdomen RLAT	DR	80	pancreas	0.04744	-1.0440E-02
Abdomen RLAT	DR	80	spleen	0.03134	-4.8620E-03
Abdomen RLAT	DR	80	stomach	0.14580	-1.3140E-02

Region	Scanner	kV	Organ	a	b
Abdomen LLAT	DR	80	adrenals	0.01174	-7.5140E-03
Abdomen LLAT	DR	80	esophagus	0.05242	-1.3830E-02
Abdomen LLAT	DR	80	kidneys	0.01947	-6.9840E-03
Abdomen LLAT	DR	80	liver	0.03078	-5.9020E-03
Abdomen LLAT	DR	80	spleen	0.00556	-1.0830E-02
Abdomen LLAT	DR	80	stomach	0.01200	-9.9500E-03

**Organ dose conversion coefficients: Parametric fits for Diagnostic DR Planar X-ray Imaging – Pediatric Patients**

Region	Scanner	kV	Organ	a	b
Head AP	DR	100	bone	0.01514	-1.7360E-03
Head AP	DR	100	brain	0.02760	-7.5070E-03
Head AP	DR	100	eye_bulbs	0.03336	-1.4030E-03
Head AP	DR	100	eye_lens	0.02765	-7.3570E-04
Head AP	DR	100	oral_mucosa	0.04486	-5.8430E-03
Head AP	DR	100	skin	0.03594	-1.1240E-02
Head AP	DR	100	bone	0.01514	-1.7360E-03

Region	Scanner	kV	Organ	a	b
Thorax AP	DR	120	bone	0.15300	-3.6520E-03
Thorax AP	DR	120	esophagus	0.09021	-5.0390E-03
Thorax AP	DR	120	heart	0.06585	-3.3860E-04
Thorax AP	DR	120	lungs	0.07097	-2.4440E-03

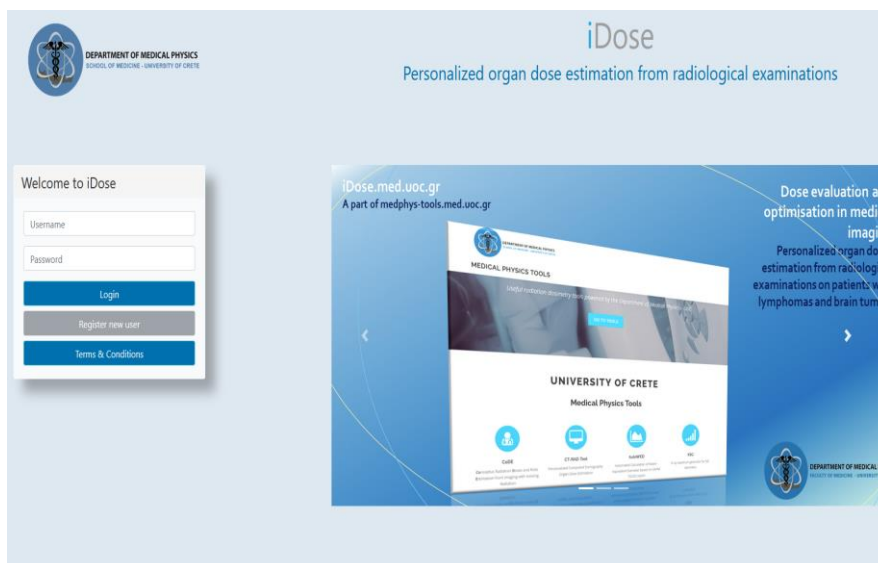
Region	Scanner	kV	Organ	a	b
Thorax LAT	DR	120	bone	0.15630	-4.5750E-03
Thorax LAT	DR	120	esophagus	0.07307	-5.3450E-03
Thorax LAT	DR	120	heart	0.05690	-1.6840E-03
Thorax LAT	DR	120	lungs	0.05900	-3.1160E-03

Region	Scanner	kV	Organ	a	b
Abdomen AP	DR	80	bladder	0.14810	-6.2650E-03
Abdomen AP	DR	80	bone	0.21190	-6.6220E-03
Abdomen AP	DR	80	kidneys	0.07861	-5.6660E-03
Abdomen AP	DR	80	liver	0.09920	-5.1710E-03
Abdomen AP	DR	80	pancreas	0.11320	-5.0270E-03
Abdomen AP	DR	80	spleen	0.09580	-6.6570E-03

## 9. Software development – iDose web calculation tool

The server-side (backend) of the calculation tool was developed using Python Django. The client-side (frontend) was implemented using HTML5, pure JavaScript, jQuery, AJAX JavaScript libraries, and Bootstrap for the CSS. jQuery is a JavaScript library designed to simplify HTML DOM tree traversal and manipulation, as well as event handling, CSS animation, and Ajax. Bootstrap is a free and open-source CSS framework directed at responsive, mobile-first front-end web development. It contains CSS- and optionally JavaScript-based design templates for forms, buttons, navigation, and other GUI components. In addition, since XML was not suitable to handle all database entries and possible future data implementations, MySQL was employed.

**iDose** (Abbrev.) – a tool for personalized organ doses estimation from radiological examinations on patients with lymphomas and brain tumors – is installed at <http://medphys-tools.med.uoc.gr> and is available upon free user registration (Figure 14).



<http://medphys-tools.uoc.gr> and <http://idose.med.uoc.gr>

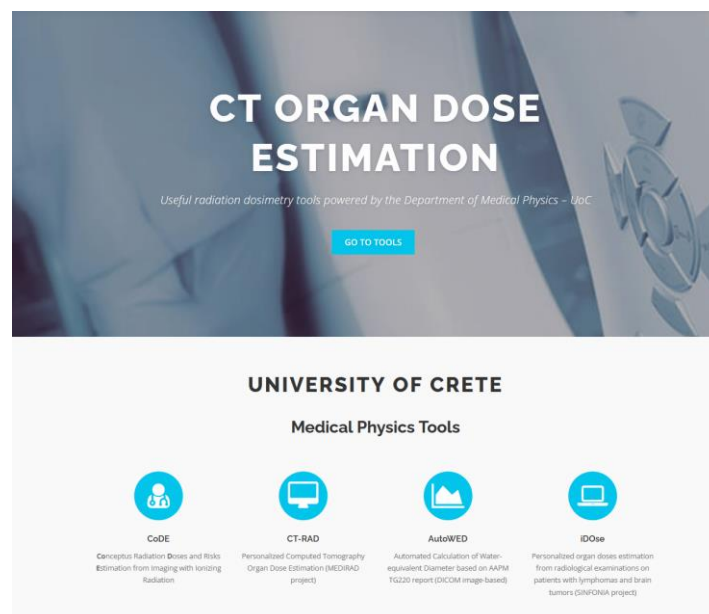


Figure 14: UoC Medical Physics tools web site and login page of iDose organ dose estimation tool, which will be located at <http://medphys-tools.uoc.gr> and [idose.med.uoc.gr](http://idose.med.uoc.gr).

Following the submission of the current deliverable report (D2.1), the dose tools will undergo continuous refinement and development throughout the project's duration. This process will be driven by users' feedback, encompassing input from UoC staff and consortium members. The aim is to address errors, enhance visuals, and improve functionality based on their valuable suggestions. Moreover, further measurements and calculations are planned to validate the precision of results from the iDose tools.

## 10. iDose web tool calculation interface

### iDose Landing Page Navigation Panel

The web-tool dose calculation code is implemented using Javascript on the client side. This reduces load from server-side requests and improve dose calculation time and web-site responsiveness. After login, the user is presented with a sleek, simple three-option integration of personalized dosimetry tools (Figure 15):

- 1. iDoseDiag:** Personalized dosimetry tool for organ doses estimation from radiological examinations on patients with lymphomas and brain tumours (as described here, in Deliverable 2.1).
- 2. iDoseRTI:** Personalized dosimetry tool for organ doses estimation from imaging in radiotherapy on patients with lymphomas and brain tumours (as described in Deliverable 2.4).
- 3. iDoseAI:** A dosimetric tool which incorporates all ML/AI algorithms from D2.1 and D2.4 for personalized dosimetry tool for organ doses prediction from examinations on patients in diagnostic radiology and radiotherapy imaging (as described in Deliverables 2.1 and 2.4).

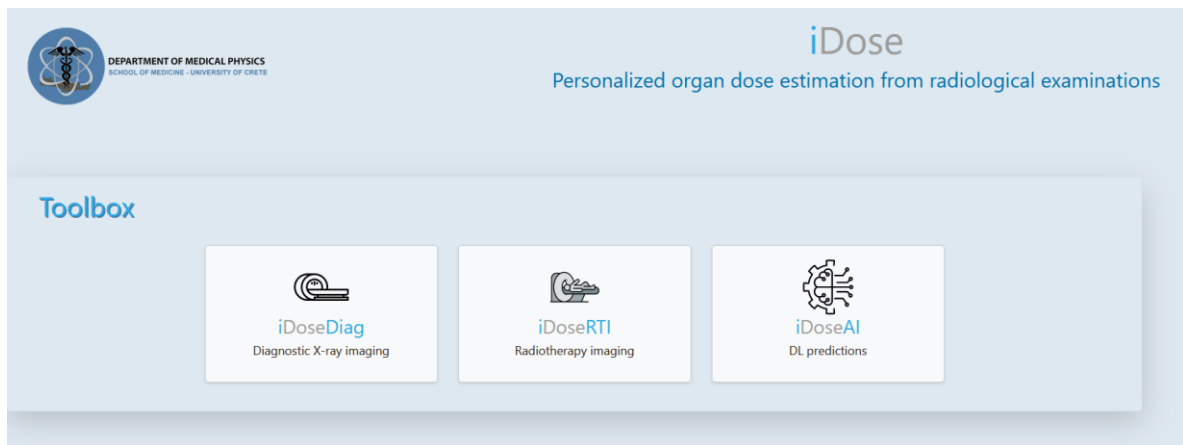


Figure 15: iDose organ dose estimation tool initial toolbox page and selection of integrated personalized dosimetry tools.

After the user leaves the iDose Landing Page, having selected the module to use, a panel is displayed encompassing all the links for access all tools according to a hierarchical structure (Figure 16). The arrangement and appearance of the panel was carefully designed for easy access to all tools, without having to move to the iDose landing page. However, the user can access these pages directly from the browser address bar, by typing:

1. [idose.med.uoc.gr/links](http://idose.med.uoc.gr/links) – for the landing page
2. [idose.med.uoc.gr/idoseddiag](http://idose.med.uoc.gr/idoseddiag) – for the iDoseDiag diagnostic page
3. [idose.med.uoc.gr/idoserti](http://idose.med.uoc.gr/idoserti) – for the iDoseRTI imaging in radiotherapy page
4. [idose.med.uoc.gr/idoseai](http://idose.med.uoc.gr/idoseai) – for the iDoseAI ML/AI algorithms page

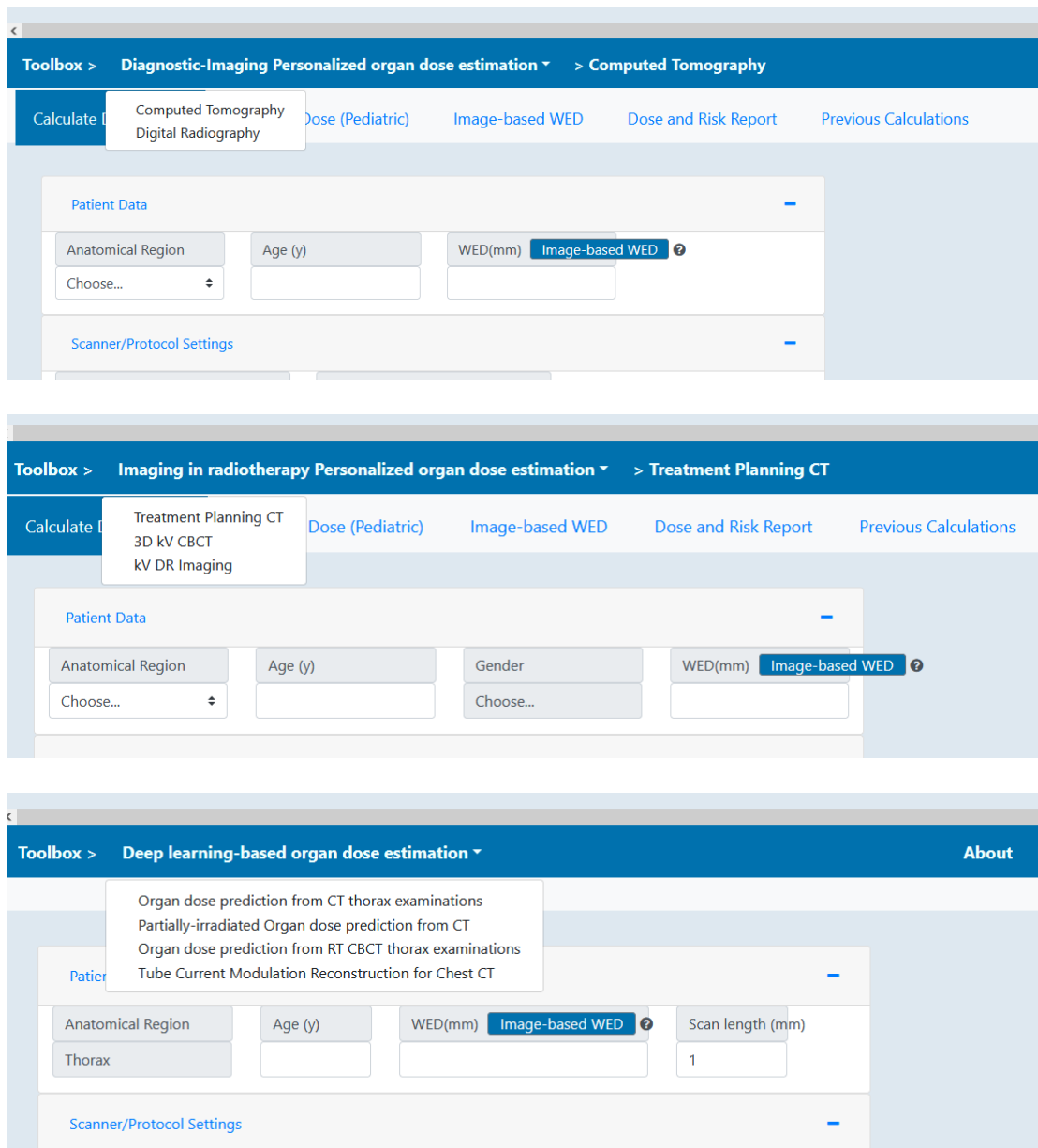


Figure 16: iDose organ dose estimation tool navigation panels for hierarchical selection of dosimetry tools.

## 11. iDose Diagnostic X-ray Imaging Module – Computed Tomography

In iDose diagnostic x-ray imaging module, organ doses from CT diagnostic scans can be estimated using the fitting parameters and dosimetric methodology explained in sections 3 to 8 (Figure 17). User input fields are organized into three groups. Each group can appear or disappear on the screen based on the preference of the user (“accordion” implementation):

- The ‘Patient Data’ group requires basic demographic input (i.e., age and gender), CT scan region (currently thorax is the only available choice), and WED, which can either be directly inserted as a number or calculated using the automatic WED calculation tool.
- In the ‘Scanner/Protocol Settings’ group, users will select the CT scanner model (three models currently available) and corresponding exposure settings (i.e., kV, mA, current modulation, beam collimation, pitch, and rotation time). Users will also select the clinical indication for the CT scan.
- In the ‘CTDI Group’, users enter the CTDI type and value for their corresponding scanner.

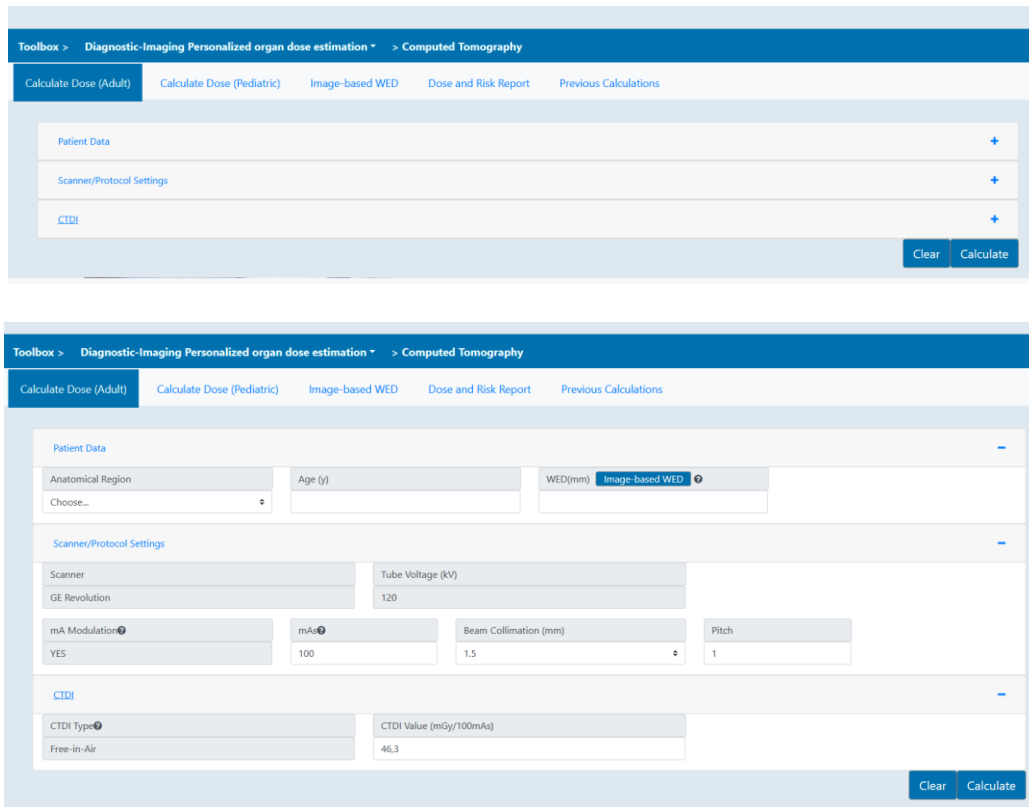


Figure 17: iDose web calculation tool interface accordion implementation overview.

Both adult and pediatric calculation tabs provide dose estimates for organs in the head/thorax/abdomen/pelvic region for patients undergoing CT examinations for various exposure settings (i.e., kV, mA, current modulation, beam collimation, pitch, and rotation time).

Patient Group submenu requires demographic data such as gender and age to be entered. This data is required for organ dosimetry and risk estimation. Water equivalent diameter is needed for correlation absorbed organ dose and patient size characteristics. WED is given in millimeters and can be entered as a value or calculated from user-uploaded CT data utilizing Image-based WEB tab.

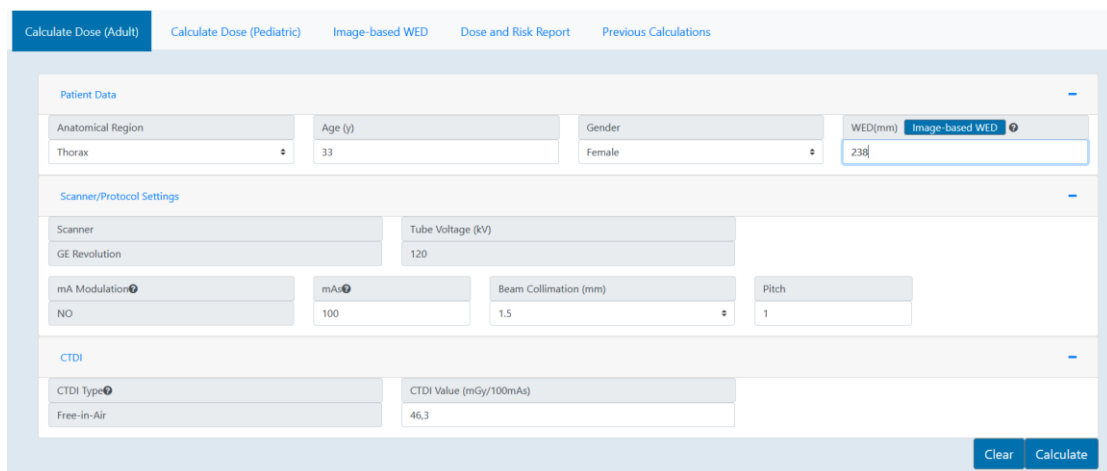


Figure 18: iDose organ dose calculation tool - main calculation tab - adults.

Scanner Group submenu requires:

- Selection of CT scanner; Currently only one scanner is available: GE Revolution.
- Tube Voltage: Currently there is one kV selectable, 120 kV.
- mA modulation: User can select if tube current modulation (TCM) or fixed tube current (NO) will be utilized or not for organ dose calculation. For the diagnostic x-ray imaging module, mA modulation is set to on (TCM), for all calculations.
- mAs: User can manually enter the mAs of the examination. For Siemens scanners, effective mAs reading from CT console should be used.
- Beam Collimation: Beam collimation in millimeters. In MDCT the actual beam collimation is not directly correlated with slice thickness. It is the length of the individual detector (or linked detector elements) acquiring data for each of the simultaneously acquired slices that limits the width of the x-ray beam contributing to that slice, this length is often referred to as detector collimation. Beam collimation depends on CT scanner and detectors configuration.
- Pitch: User can select pitch of the examination.
- Rotation time: User can specify time (in seconds) in which a full gantry rotation is performed.

CTDI Group submenu requires the user to enter CTDI type and value for their corresponding scanner. CTDI values can be entered in their CTDI-free-in-air form (Figure 18).

## 12. iDose Diagnostic X-ray Imaging Module – Digital Radiography

In iDose diagnostic x-ray imaging module, organ doses from conventional diagnostic scans can be estimated using the fitting parameters and dosimetric methodology explained in sections 3 to 8.

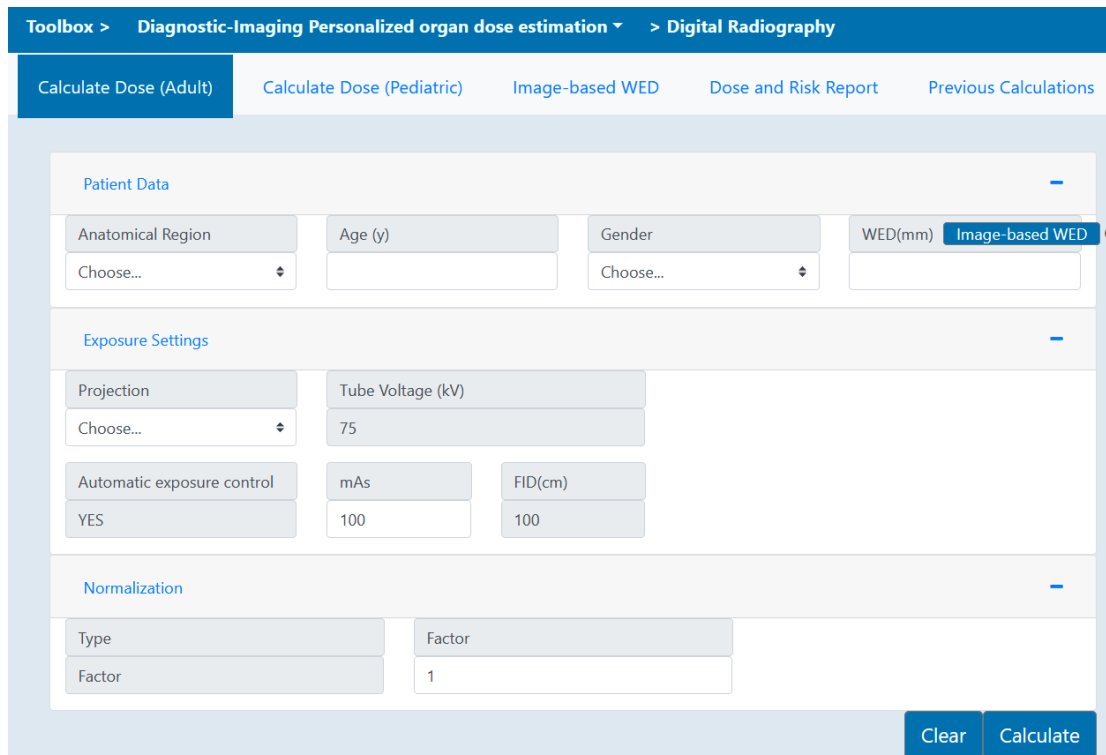


Figure 19: iDose organ dose calculation tool - main calculation tab - adults.



Both adult and pediatric calculation tabs provide dose estimates for organs in the head/thorax/abdomen-pelvic region for patients undergoing conventional planar (DR) examinations for various predefined exposure settings.

Patient Group submenu requires demographic data such as gender and age to be entered. This data is required for organ dosimetry and risk estimation. Water equivalent diameter is needed for correlation absorbed organ dose and patient size characteristics. WED is given in millimeters and can be entered as a value or calculated from user-uploaded CT data utilizing Image-based WEB tab. In addition, the tool will suggest a value for WED according to patient's BMI, if no image is available for WED calculations.

Exposure settings submenu requires:

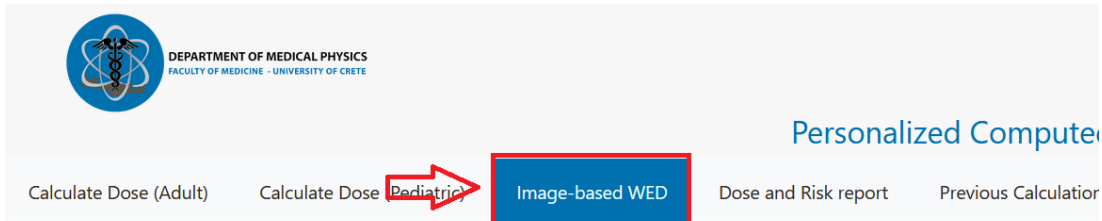
- Selection of anatomical region: Head, Thorax, abdomen pelvis
- Tube Voltage: Tube voltage is fixed for each radiological examination (eg 125kVp for thorax, 80 kVp for head, see table 4, section 3).
- mAs: tube load is fixed for each radiological examination and represents the most commonly mAs used with AEC; however, user can alter tube load to calculate organ dose for different exposure settings.
- FID: Fous-to-Image Receptor-Distance is fixed and represents mostly used distance for each radiological examination (FID=180cm for thorax, FID=100 cm for tabletop examinations).

## 13. Automatic Imaged-Based Water-equivalent diameter (WED) calculation module

Accurate WED determination requires detailed delineation of the patient body outline on the CT slice without including the CT couch/table. Within iDose, an automatic module for calculation of WED based on user-uploaded CT scans was developed. The algorithm is based on morphological operations applied on each image slice. A square structuring element with heuristically determined size equal to 12 pixels was used to perform morphological opening. This step effectively removed small structures in the vicinity of the body and preserved the body shape and size. The next step was conversion of the image to binary using Otsu's method to determine the single HU threshold between background and any other structure [16, 17]. During this step, the couch is usually removed from the image without affecting the body size or shape. Lungs and other low-density tissues are likely to produce empty space (holes) in the binarized image within the region defined by the body shape. This empty space was filled by detection of zero value locations that were not connected with the image borders. In the final step, non-zero areas that were not connected were identified and the largest area was kept (i.e. the body) – this step was rarely required but nevertheless performed (see figure below).

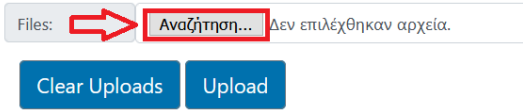
For imaged-based WED calculation, the user is prompted with an interface to upload a single DICOM image or a DICOM series as a group of images for the WED calculation (of each image/slice) to AAPM TG220 formulation. No images and DICOM header information are stored after exiting the Imaged-Based calculation tab, so there is no risk of sharing sensitive patient data.

After image upload and processing, WED and tube current values for each uploaded DICOM image/series are presented and the user can select which WED value will be used/transferred to the organ dose calculation tab. Users can use average, median, or WED value for a specific slice in this tool.



Automated Calculation of Water-equivalent Diameter (WED) Based on AAPM Task Group 220 report.

Using this tool, users can upload a single DICOM image or a DICOM series (stack) in order to calculate/select the WED to be used for dosimetric calculations.



Automated Calculation of Water-equivalent Diameter (WED) Based on AAPM Task Group 220 report.

Using this tool, users can upload a single DICOM image or a DICOM series (stack) in order to calculate/select the WED to be used for dosimetric calculations.

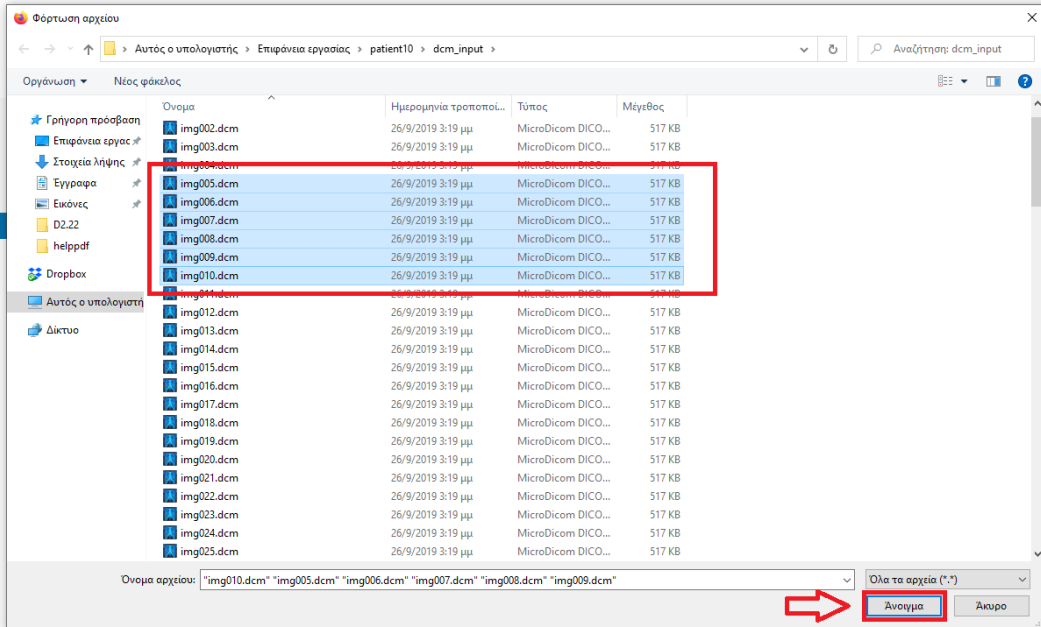
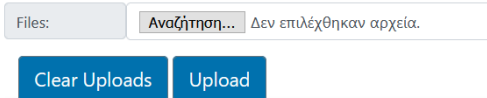


Figure 20: Image-based WED tool inside iDose organ dose calculation tool with image upload capability.

## WED Results:

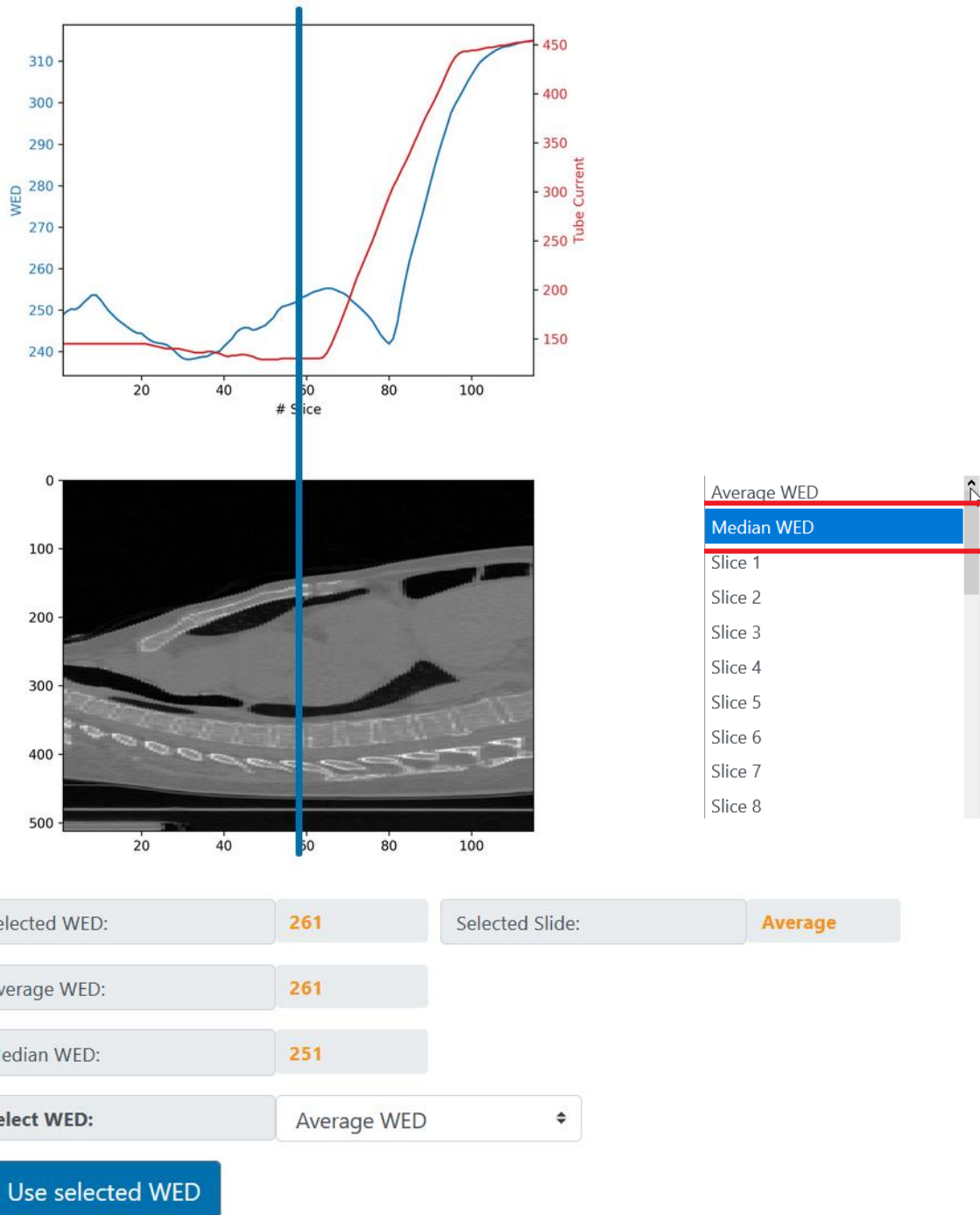


Figure 21: Image-based WED calculation from user-supplied DICOM series inside iDose organ calculation tool.

## 14. AI algorithm development – Rapid estimation of patient-specific organ doses from thoracic CT examinations using a deep learning network

Traditional methods to estimate patient dose, rely on standardized phantom-based measurements using TLDs or other detectors which provide either point or 2D estimates of dose. Although these methods clearly depict dose distributions from actual measurements, they lack on doing so on real patients. MC based dose estimation techniques have increasingly been applied as more computing power became available. However, MC computations rely on a computerized representation of the scanner characteristics and the patient, usually through a set of CT images. With the advent of AI in medical applications, solutions that provide accurate dose estimations based on deep-learning algorithms have emerged. The training difficulty and the need for possible additional algorithms for various steps of the dose estimation procedure (e.g., image segmentation) may append challenges in the implementation of such a workflow.

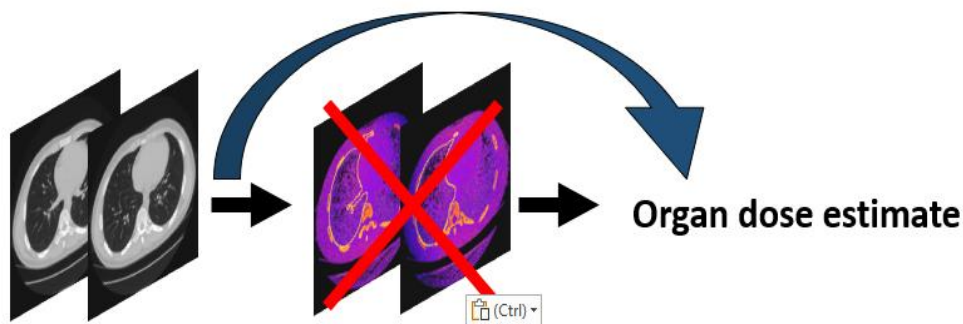


Figure 22: AI-based personalized organ dose estimation scheme without MC/segmentation implementation.

A probable exploitation of the initial dose distributions obtained through MC computations, is to create a shortcut to the organ dose estimation procedure: Initially calculate organ doses and then train an NN to directly provide these organ dose values. Furthermore, instead of using a CT image as input, specific parameters included in or derived from the CT images can be associated with patient-specific organ doses and used as independent variables. This adaptation bypasses the difficulties and steps associated with 3D dose distribution generation through complex deep learning NN (Figure 22).

### Patient data collection & MC software parametrization

Volumetric image data from 95 adult individuals undergoing thorax CT examinations with were collected. Another dataset of 19 patients, not used during training and validation with similar characteristics and exclusion criteria were collected for algorithm testing. Patient CT scans were performed with predefined protocols suitable for thoracic imaging in all scanners. In a standard thoracic protocol, the scanned anatomy is defined as just before the apices to just above adrenals. Esophagus, breast, and heart were manually delineated by an experienced operator. Patient surface, bone structures and lungs were automatically delineated as described in section 6.

Scanner-specific dose estimation required the parameterization of the MC software according to operating and physical characteristics of each scanner considered. The CT scanner model were based on data for x-ray beam spectra, beam shaping devices (bow-tie filters) and geometrical specifications. The required data were provided by the manufacturer and later compiled and converted to input parameters suitable for ImpactMC MC software. The CT scan of each patient was used as input volume to perform dosimetric

computations at 120 kV. Separate computations were performed for modulated and fixed current. The MC software output after each computation was in the form of three-dimensional (3D) dose distribution. There is a pixel-to-pixel correspondence between the CT images and corresponding dose images. The output dose was normalized to CT dose index in free air ( $CTDI_{air}$ ). A representation of organ dose estimation scheme with MC/segmentation implementation for constructing ground truth data used in NN training is depicted in Figure 23.

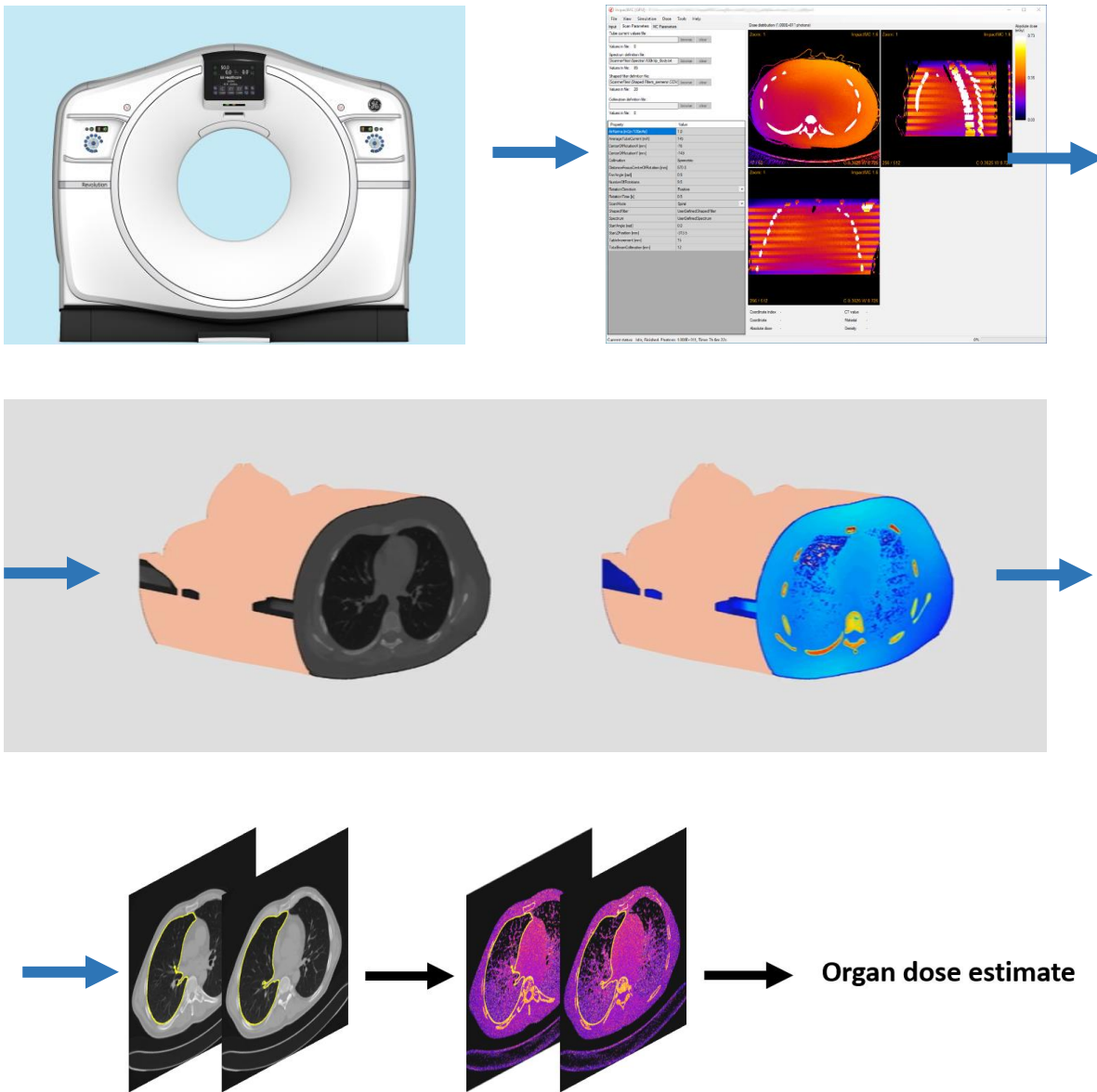


Figure 23: Personalized organ dose estimation scheme with MC/segmentation implementation for constructing ground truth data used in NN training.

### Deep-learning network architecture and training

The deep-learning network architecture was implemented in MATLAB® using the Deep Learning Toolbox™. The network was composed of three fully connected hidden layers with rectified linear activation functions (ReLU). The number of nodes in each hidden layer was 200, 100 and 50 respectively. The final layer was a regression layer. The independent variables were the scan length, the average current value (mAavg) and the average WED value for each patient. Scan length and mAavg can be readily calculated from the DICOM header of the CT images. WEDavg was calculated as described in section 13. The dependent variable was total dose per organ, estimated through Monte Carlo simulations for each patient. A neural network was trained separately for each organ included in this work, namely, lungs, bone, heart, and esophagus after applying 10-fold cross-validation to the dataset. The metrics used to determine training convergence and performance was accuracy (defined as 1-validation loss). The networks were trained for 500 epochs. Training and validation datasets were drawn from the patients’ dataset. During the 10-fold cross-validation, the dataset was split to 90% and 10% training and validation respectively. Independent testing of the algorithm was performed on the 19 patients’ dataset that was not used for training nor validation (Figure 24).

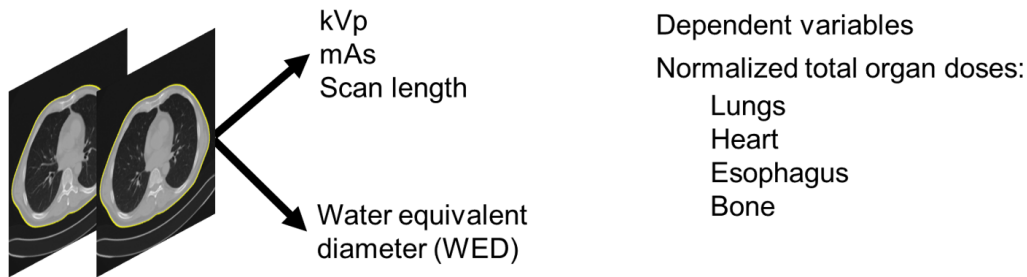


Figure 24: DL-network architecture dependent and independent variables.

In Table 6, the average relative difference between MC estimated and deep learning network generated organ dose values is demonstrated along with associated error range. In Figs. 25-28, organ dose estimated values generated using the deep learning algorithm (dashed red line) were compared with Monte Carlo based organ dose values for each organ considered in this work, namely bones, esophagus, lung, and heart. Perfect agreement is depicted with a red line ( $R^2=1$ ).

The time required to generate predictions with the deep-learning network was less than a second.

There was good agreement between the deep learning algorithm and Monte Carlo organ dose estimates in the training and the test dataset. The relative difference in any organ was on average within 2% in the training dataset and 5% in the test dataset (Figure 29). The magenta lines indicate the 25% relative error limit. The red dashed line is the average error (Ravg=5.1%).

Organ	Average Relative Error	Standard Deviation
Bones	-0.4%	8.0%
Esophagus	-1.6%	6.9%
Heart	-1.5%	7.6%
Lungs	-1.0%	10.5%

Table 6: Average error and standard deviation between deep learning network and Monte Carlo estimated organ-dose values.

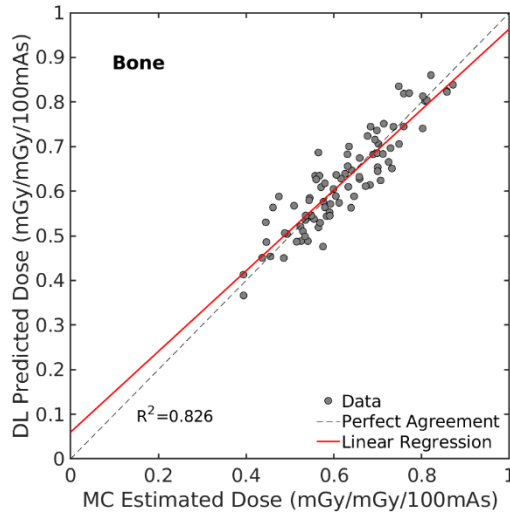


Figure 25: Plot of DL-predicted dose against Monte Carlo estimated dose for bone tissue. Linear regression is show with dashed line ( $R^2=0.826$ ). Perfect agreement is depicted with red line.

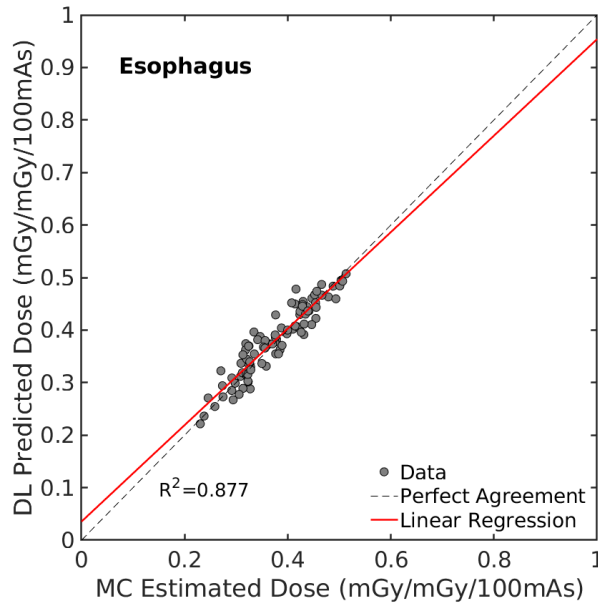


Figure 26: Plot of DL-predicted dose against Monte Carlo estimated dose for esophagus tissue. Linear regression is show with dashed line ( $R^2=0.877$ ). Perfect agreement is depicted with red line.



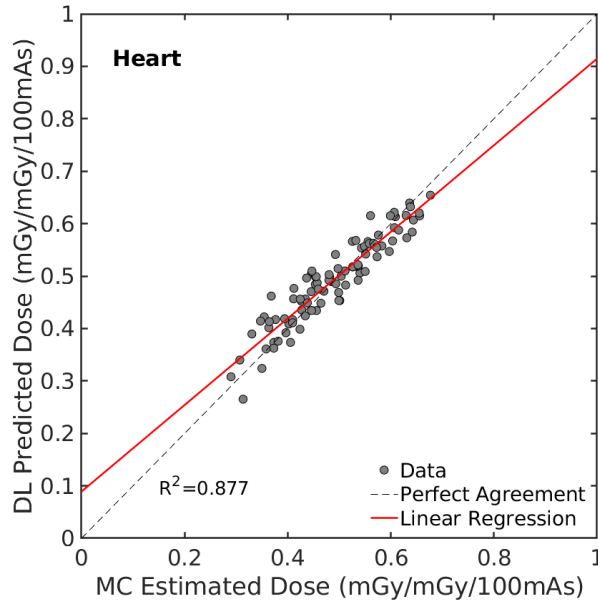


Figure 27: Plot of DL-predicted dose against Monte Carlo estimated dose for heart tissue. Linear regression is show with dashed line ( $R^2=0.877$ ).

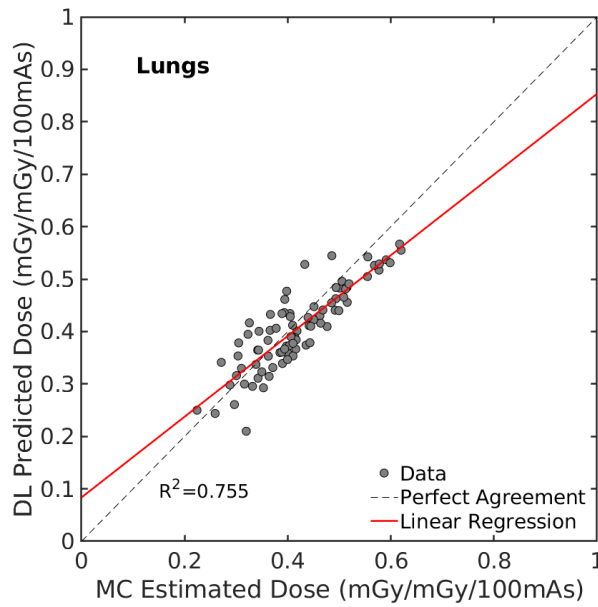


Figure 28: Plot of DL- predicted dose against Monte Carlo estimated dose for lung tissue. Linear regression is show with dashed line ( $R^2=0.775$ ). Perfect agreement is depicted with red line.



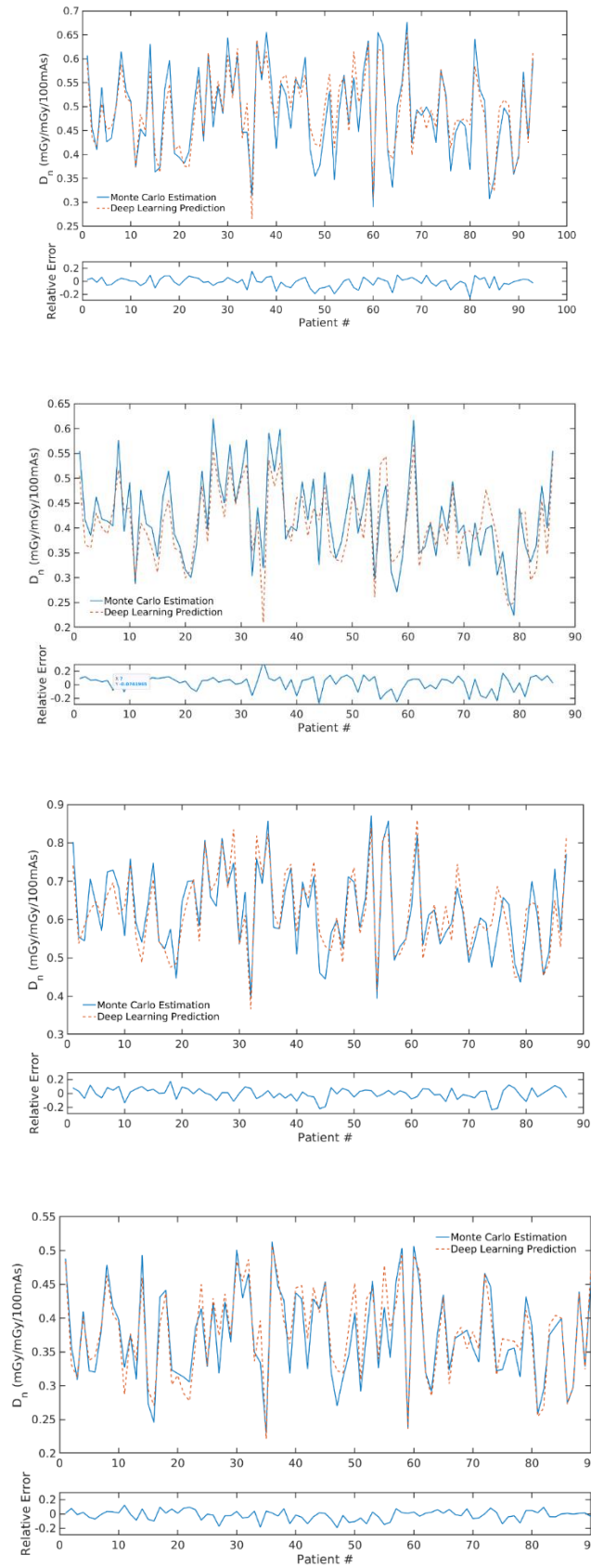


Figure 29: Relative prediction error between deep-learning predicted and Monte Carlo estimated organ doses values in the test dataset (bones, oesophagus, heart, lung are depicted).

A further advantage of the method is the direct estimation of organ dose values for a specific patient based on input data that are readily available on the DICOM header of the CT images and can be applied during or immediately after patient imaging. The direct estimation of organ dose implies that the DL algorithm does not generate two- or three- dimensional dose images that would have required the application of a segmentation method to delineate the organ in question and then extract the relevant dose. Skipping the generation and segmentation of images, two computation steps are avoided that would have increased the final uncertainty in the calculated dose and the complexity of the deep learning algorithm. A potential workflow in a clinical setting would include the following steps without user interaction: a) the patient CT scan is acquired; b) the WED values are automatically calculated from patient images; c) scan length and tube-current are extracted from DICOM header; d) WED, scan length and tube current values inserted in the deep-learning network and organ dose values predicted.

## 15. AI algorithm development – Partially-irradiated liver dose estimation through a deep learning regression NN

Efforts have been made to develop robust methodologies to allow direct estimation of organ doses from patients undergoing CT exams. New metrics for CT dose quantification have been proposed, such as the effective diameter and water-equivalent diameter, which are adopted to assess the size specific dose estimates (SSDE). Estimation of organ dose values is not a trivial task. Various approaches have been adopted over the past decades for the estimation of organ doses such as direct measurements with different kinds of dosimeters, anthropomorphic phantoms and calculations using Monte Carlo methods combined with computational human phantoms.

Monte Carlo simulations generate accurate 3D dose distributions which are useful to estimate organ doses of individual scans. Usually, they are based on the parameters of a scan (x-ray spectrum and geometry) and in patient-specific cases utilize CT reconstructed data, to calculate the dose deposited in each single volume element (voxel) considering all relevant photon interaction processes. MC output comprises of parametric dose images in which every voxel carries the normalized dose (to CTDI) of the initial image grid. Methods for scanner-specific and patient-specific, organ-dose estimation are based on a procedure that combines MC computational techniques and patient CT scans. The procedure is usually composed of five steps: (a) collection of suitable patient CT scans; (b) determination of scanner parameters; (c) Monte Carlo dosimetric computations; (d) three-dimensional (3D) patient-specific dose distribution output and (e) correlation between dose and patient characteristics.

Time consuming dose computations are based on scanner-specific data for x-ray beam spectra, beam shaping devices (bow-tie filters) and geometrical specifications. Dose is calculated on a per image voxel basis and output comprises of parametric dose images in which every voxel carries the dose normalized to CTDI. Moreover, organ dose information must be extracted from 3D dose distributions through laborious delineation and segmentation of specific organ/tissue structures (Figure 30).

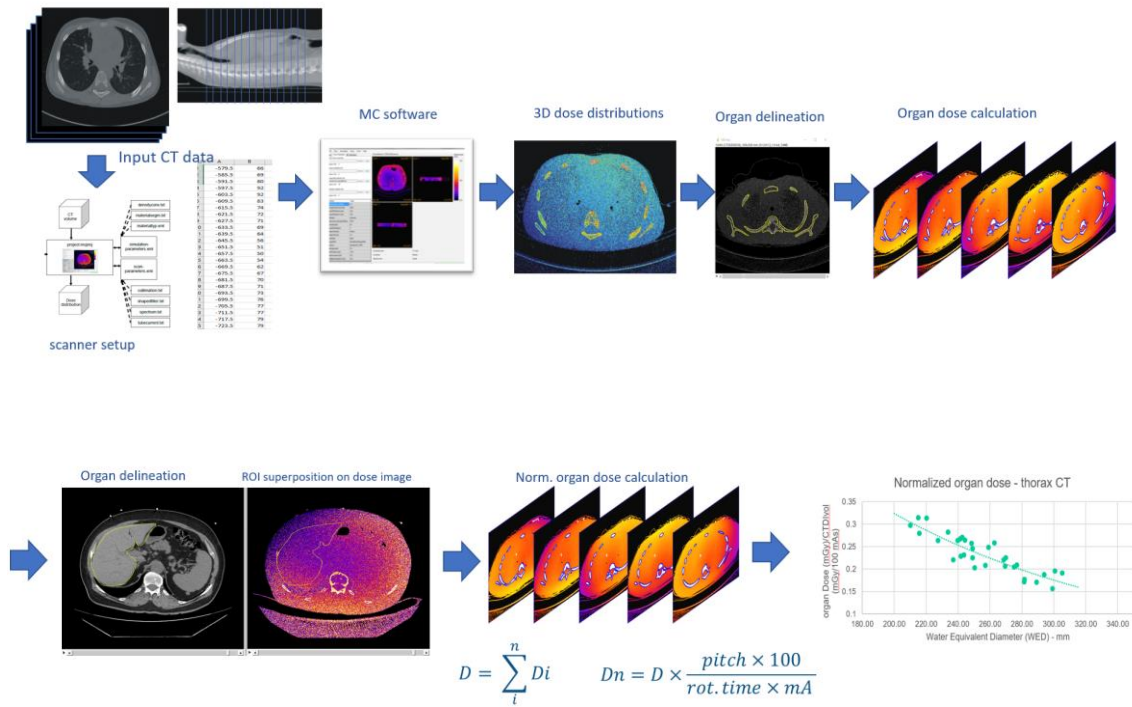


Figure 30: Schematic representation of a MC-based organ estimation methodology.

Furthermore, patient-specific MC organ dose estimation using patient’s CT images is limited to the scanning length and does not allow dose estimation for partially exposed organs or organs located outside the imaged region. For example, for thorax CT scans, liver is partially exposed during the scan, so CT data for calculating energy deposition to the liver, and liver volume to estimated dose to the liver (mGy/mass) are inevitably absent (Figure 31).

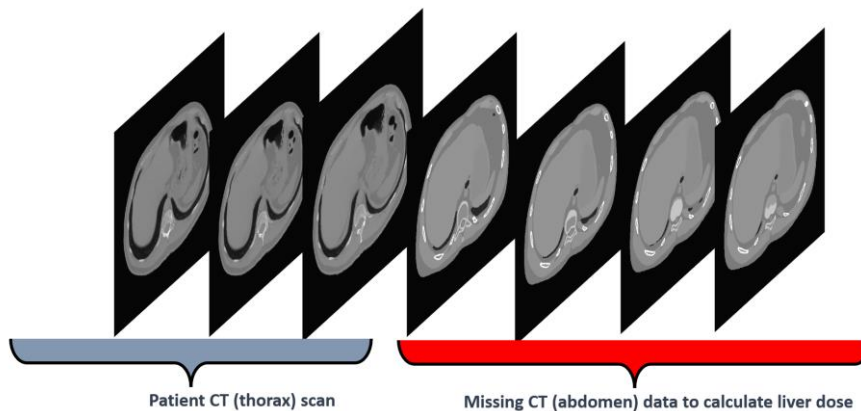


Figure 31: Missing CT abdomen data for MC-based organ calculation.

Acquisition parameters and demographic data were recorded for a series of 200 patients of various sizes referred for thorax CT. In CT exposures, patients’ liver was always partially irradiated since CT thorax Z-axis coverage encompasses only thoracic structures, commonly starting just above apices and ending just above patient’s adrenals.

Patients' size-specific parameters, such as chest/torso and organ dimensions, age, and sex, were used to construct virtual models of the patients' anatomy using extended Cardiac-Torso (XCAT) anatomical phantom framework to resemble the patients as much as possible. The XCAT series encompasses a vast population of phantoms of varying ages from newborn to adult, each including parameterized models using nonuniform rational b-spline (NURBS) surfaces based on the Visible Male and Female anatomical datasets from the National Library of Medicine. With great flexibility in the XCAT's design, any number of body sizes, different anatomies, cardiac or respiratory motions or patterns, patient positions and orientations, and spatial resolutions can be simulated (Figure 32).

These computational phantoms, besides thorax data, contain abdomen data, not present in routine thorax CT, which were used to complement body areas for the simulations and facilitate energy deposition on non-irradiated liver tissue. MC simulations were performed to estimate the liver dose, used as ground truth for the development of the deep-learning model. Scan length was calculated from the DICOM header of the CT images. WED was calculated as described in section 13.

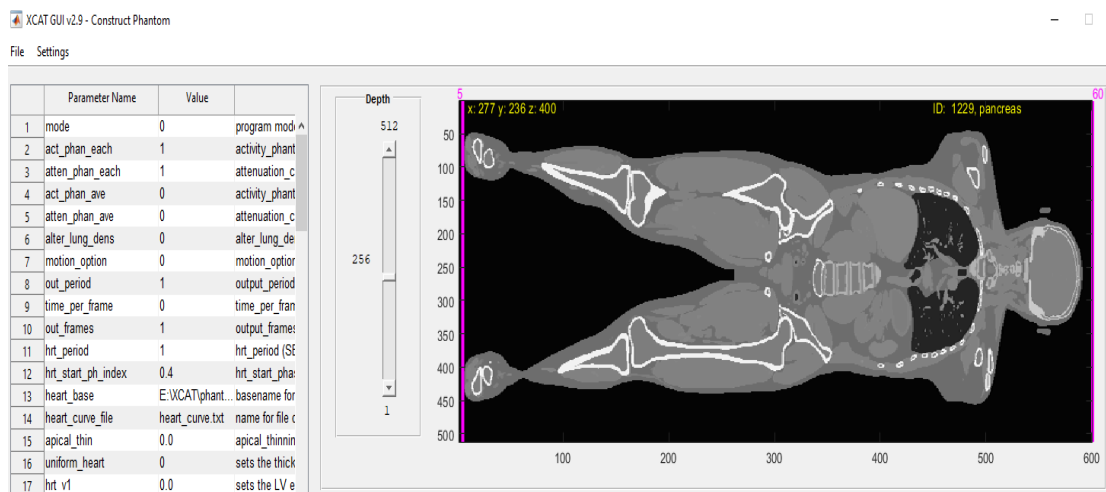


Figure 32: Highly detailed whole-body anatomical family of XCAT digital phantoms.

An artificial neural network, which functions as a regression model, was developed, and optimized, to predict liver doses based on features such as dimensions of the XCAT models (resembling real patients), scanning length, and WED.

The network was composed of three fully connected hidden layers with rectified linear activation functions (ReLU). The number of nodes in each hidden layer was optimized through separate hyperparameters optimization strategies (No of layers, learning rate, dropout rate through Hyperband tuning). The final layer was a regression layer. The independent variables were the scan length, thorax circumference, chest and abdomen width and the average WED value for each patient/model.

Data preprocessing and splitting was applied for optimization and testing purposes. Training and validation datasets were drawn from the patients' dataset. The dataset was split to 70% and 30 % training and validation respectively. Independent testing of the algorithm was performed on the dataset that was not used for training nor validation.

The dependent variable was normalized dose of the liver structure, as estimated through Monte Carlo simulations for each patient model. The metrics used to determine training convergence and performance was accuracy (defined as 1-validation loss). The networks were trained for 200 epochs using early stopping before reaching the specified maximum number of epochs to avoid overfitting to the data, thus improving the network generalization.

## Optimization strategies

Hyperparameters are configurations that determine the structure of machine learning models and control their learning processes. They shouldn't be confused with the model's parameters (such as the bias) whose optimal values are determined during training. Hyperparameter optimization is an integral part of deep learning as a machine learning project is crucially dependent on the choice of good hyperparameters (Figure 33).

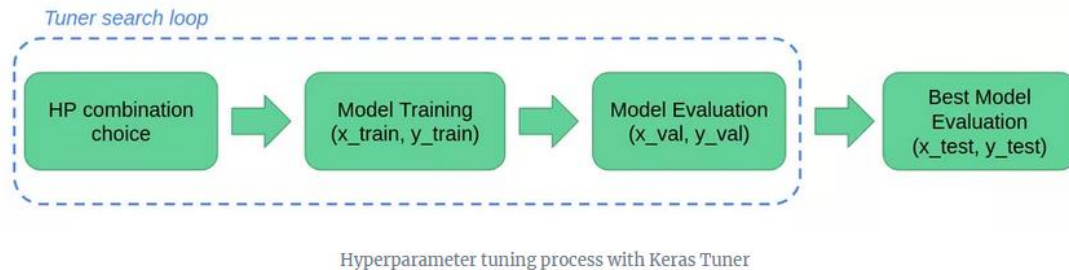


Figure 33: Optimization strategy of a neural network architecture.

The two main types of hyperparameters are the model hyperparameters (such as the number and units of layers) which determine the structure of the model and the algorithm hyperparameters (such as the optimization algorithm and learning rate), which influences and controls the learning process. Standard hyperparameters for training neural nets include:

1. Number of hidden layers
2. Number of units for hidden layers
3. The dropout rate - A single model can be used to simulate having many different network architectures by randomly dropping out nodes during training.
4. Activation function (Relu, Sigmoid, Tanh) - defines the output of that node given an input or set of inputs.
5. Optimization algorithm (Stochastic Gradient descent, Adam Optimizer, RMSprop, etc.) - tools for updating model parameters and minimizing the value of the loss function, as evaluated on the training set.
6. Loss function - a measurement of how good your model is in terms of predicting the expected outcome.
7. Learning rate - controls how much to change the model in response to the estimated error each time the model weights are updated.
8. Number of training iterations (epochs) - the number times that the learning algorithm will work through the entire training dataset.
9. Batch size - this hyperparameter of gradient descent that controls the number of training samples to work through before the model's internal parameters are updated.

Depending on the performance of the model after initial training, these values are repeatedly adjusted to improve the model, until a combination of values that produces the best results is chosen. The process of adjusting hyperparameters to obtain the right set of values that optimizes the performance of machine learning models is known as Hyperparameter Tuning. Tuning hyperparameters could be challenging in deep learning. This is mainly due to the different configurations that need to be rightly set, several trials of re-adjusting these values to improve the performance and the poor results that arise from setting sub-optimal values for the hyperparameters. Manually fine-tuning hyperparameters is often laborious, time-consuming,

sub-optimal and inefficient for managing computing resources. An alternative approach is to utilize scalable hyperparameter search algorithms such as Bayesian optimization, Random Search, and Hyperband (Figure 34). Keras Tuner is a scalable Keras framework that provides these algorithms built-in for hyperparameter optimization of deep learning models ([16], also see Appendix A).

*Random Search Optimization Algorithm*

The algorithm sets up a grid of hyperparameter values and selects *random* combinations to train the model where the number of search iterations is set based on time and resources. Random search is much more efficient than grid search, where all the possible combinations from the grid are tried until the best combination is found. Although grid search finds the optimal values of hyperparameters, the random search usually considers a good enough combination in far fewer iterations (Figure 35).

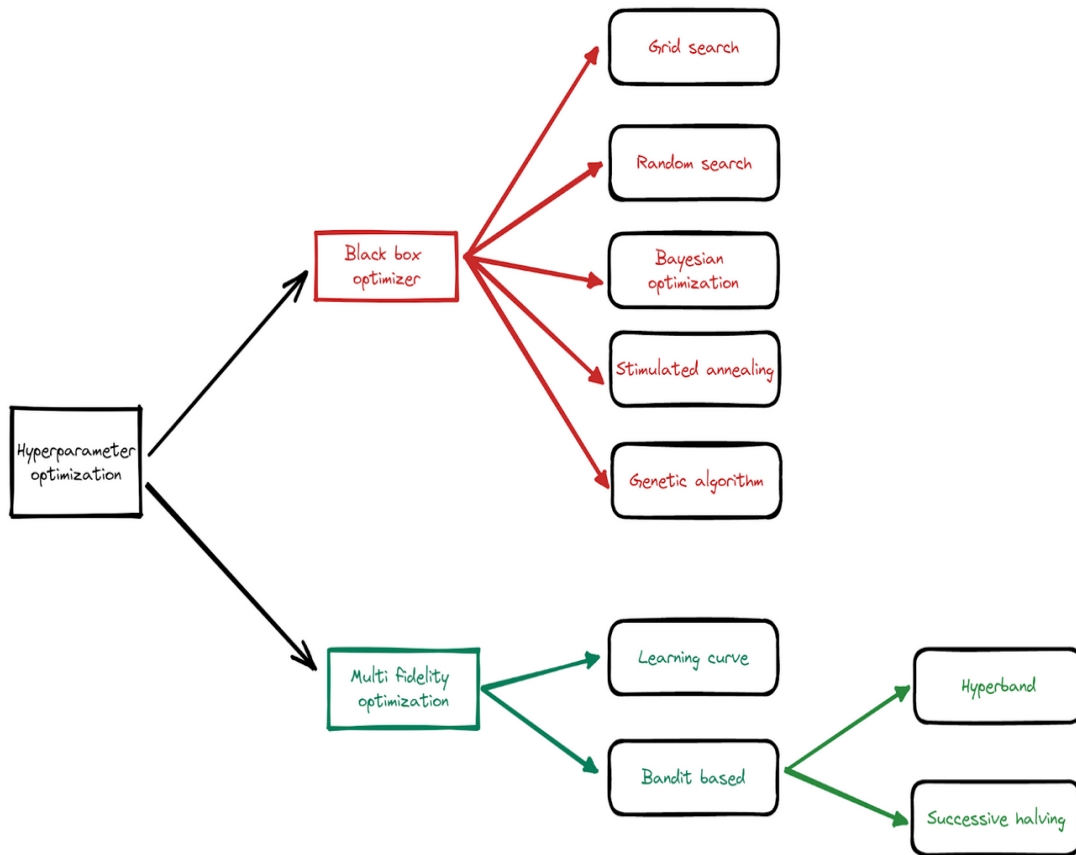


Figure 34: Hyperparameter tuning optimization algorithms.



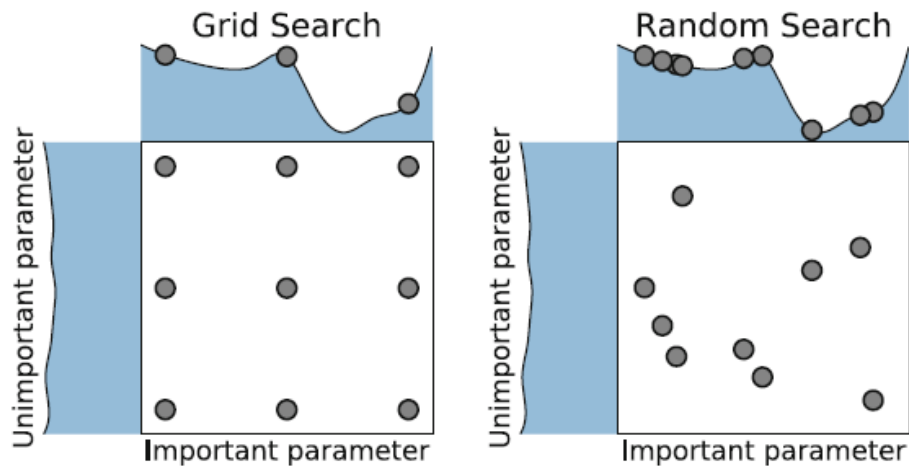


Figure 35: Comparison of grid search and random search for minimizing a function with one important and one unimportant parameter (adapted from [17]).

### Bayesian Optimization Algorithm

Bayesian optimization is an iterative algorithm with two key ingredients: probabilistic surrogate model and an acquisition function to decide which point to evaluate next. In each iteration, the surrogate model is fitted to all observations of the target function made so far. Then the acquisition function, which uses the predictive distribution of the probabilistic model, determines the utility of different candidate points, trading off exploration and exploitation. Bayesian optimization aims to become less wrong with more data inputs done by continually updating the surrogate probability model after each objective function's evaluation epoch. The algorithm builds a surrogate probability model of the objective function and finds the hyperparameters that perform best on the surrogate. The hyperparameters acquired are applied to the actual objective function, and the algorithm is run till the desired results are not achieved.

### Hyperband Optimization Algorithm

Hyperband is an optimized variation of random search which uses early stopping to speed up the process. The underlying principle of the procedure exploits the idea that if a hyperparameter configuration is expected to be the best after a considerable number of iterations, it is more likely to perform after a small number of iterations. It allocates resources using a logical early-stopping technique, allowing it to test orders of magnitude more configurations than black-box processes such as Bayesian optimization methods.

The capacity of Hyperband to adapt to unknown convergence rates and the behavior of validation losses as a function of the hyperparameters was proved by the developers in the theoretical study. Furthermore, for a range of deep-learning and kernel-based learning issues, Hyperband is 5 to 30 times quicker than typical Bayesian optimization techniques. In the non-stochastic environment, Hyperband is one solution with properties like the pure-exploration, infinite-armed bandit issue.

In order to develop more efficient search methods, Bayesian optimization approaches that focus on optimizing hyperparameter configuration selection have lately dominated the subject of hyperparameter optimization. By picking configurations in an adaptive way, these approaches seek to discover good configurations faster than typical baselines such as random search. The goal of an orthogonal approach to hyperparameter optimization is to accelerate configuration evaluation. These methods are computationally adaptive, providing greater resources to promising hyperparameter combinations while swiftly removing bad ones. The size of the training set, the number of features, or the number of iterations for iterative algorithms are all examples of resources.

These techniques seek to analyze orders of magnitude more hyperparameter configurations than approaches that evenly train all configurations to completion, hence discovering appropriate hyperparameters rapidly. The hyperband is designed to accelerate the random search by providing a simple and theoretically sound starting point.

### Bayesian optimization

A probability-based model

Learns an expensive objective function by past observation.

Bayesian optimization is only applicable to continuous hyperparameters, not categorical ones.

### Hyperband

A bandit-based model

In each given situation, the goal is to reduce the simple regret, defined as the distance from the best choice, as rapidly as feasible.

Hyperband can work for both continuous and categorical hyperparameters

Table 7: Bayesian optimization vs Hyperband optimization algorithm properties.

### Data preprocessing and data splitting for training and validation purposes

```
#standard data preprocessing for data normanilization
min_max_scaler = preprocessing.MinMaxScaler()
X_scale = min_max_scaler.fit_transform(X)
X_train, X_val_and_test, Y_train, Y_val_and_test = train_test_split(X_scale,
Y, test size=0.3)
```

### Hyperband Hyperparameters optimization/tuning:

```
def build_model (hp):
    model = tf.keras.Sequential()

    for i in range(hp.Int('layers', 3, 6)):
        model.add(tf.keras.layers.Dense(units=hp.Int('units_' + str(i), 16, 512,
step=16),
activation=hp.Choice('act_' + str(i),
['relu', 'selu'])))

    model.add(Dense(1, kernel_initializer='normal', activation='linear'))
    hp_learning_rate = hp.Choice('learning_rate', values=[1e-2, 1e-3, 1e-4])

    optimizer = hp.Choice('optimizer', ['adam', 'sgd', 'rmsprop'])
    model.compile(optimizer=optimizer, loss=msle, metrics=[msle])

    return model
```



```
nEpochs = 40

tuner = kt.Hyperband(build_model,
                    max_epochs=nEpochs,
                    objective='val_loss',
                    directory='keras_tuner',
                    project_name='keras_tuner_1',
                    #max_trials=15,
                    overwrite = 'false'
                    )

tuner.search(X_train, Y_train, epochs=nEpochs, batch_size=2,
            validation_data=(X_val, Y_val))
```

Another problem with training neural networks is in the choice of the number of training epochs to use. Too many epochs can lead to overfitting of the training dataset, whereas too few may result in an underfit model. The model loss v/s Epochs graph shows how the Training loss get reduced with increase in the number of Epochs. The losses reduced as the Epochs increases, but they become saturated after several epochs and a further reduction in loss are negligible. An early stopping method which monitors `val_loss` was used (Figures 36-38).

However, the first sign of no improvement may not be the best time to stop training. This is because the model may get slightly worse before getting much better. We can account for this by adding a delay to the trigger in terms of the number of epochs on which we would like to see no improvement. This can be done by setting the “*patience*” argument.

```
#evaluation of the best model (model with optimal parameters)

stop_early = tf.keras.callbacks.EarlyStopping(monitor='val_loss',
                                             patience=50)

hist = best_model.fit(X_train, Y_train, batch_size=1, epochs=200,
                    validation_data=(X_val_and_test, Y_val_and_test), verbose=1,
                    callbacks=[stop_early])
```

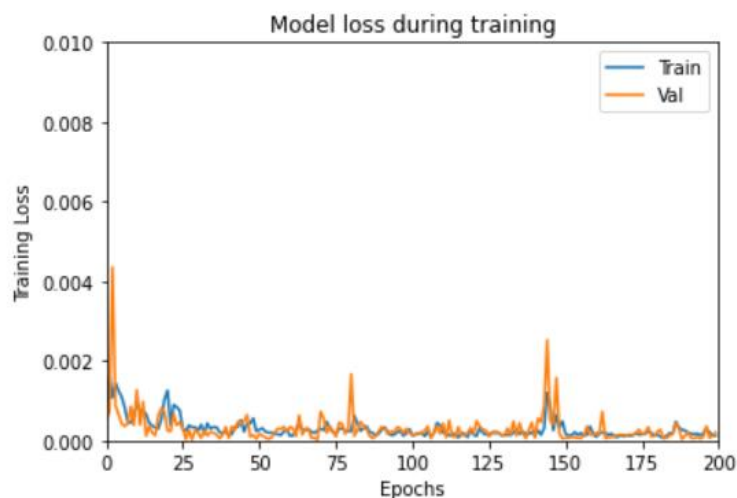


Figure 36: Training model loss v/s Epochs graph.

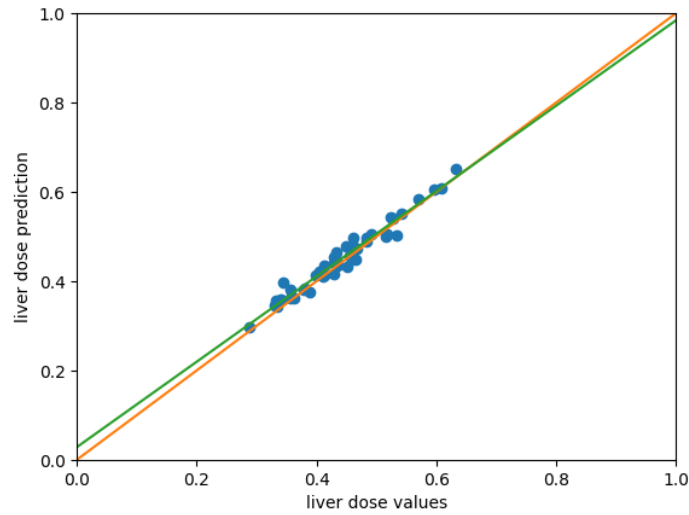


Figure 37: Prediction on the train dataset based on the best model.

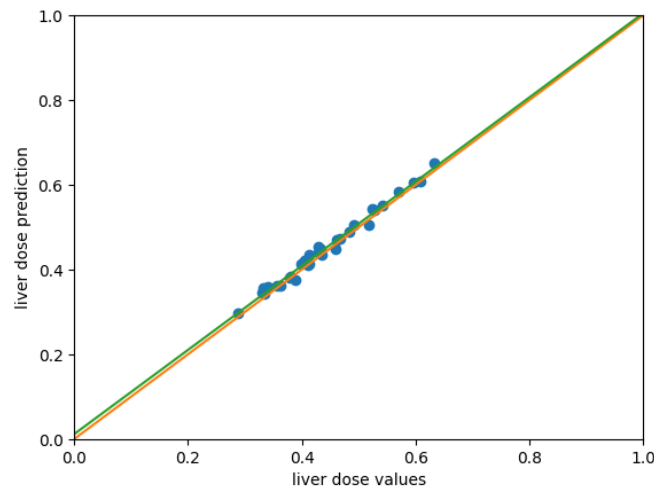


Figure 38: Prediction on the test dataset based on the best model.

## 16. AI algorithm development – Tube Current Modulation Reconstruction from Chest CT Images Using Deep-learning Regression Algorithms

Patient-specific organ-dose estimation from CT examinations can be estimated with high accuracy using Monte Carlo computations. The process usually requires specific patient models, i.e., voxelized phantoms based on CT scans, and scanner-specific details (e.g., geometry, mA modulation). Tube-current modulation can be retrieved retrospectively from DICOM headers of each reconstructed slice, albeit it merely represents an average of the transverse and angular modulation.

CT dose optimization requires estimation of organ dose for a specific protocol and scanner. Voxelized phantoms of specific patients may be constructed from previous scans acquired at different CT scanners. As such, tube-current modulation data for specific patients may not be available for the scanner at hand.

Estimation of patient-specific tube-current modulation patterns for a specific scanner from patient images acquired at a different CT scanner may pose a valid and accurate solution to this challenge. In this work we propose the use of size-specific metrics (such as water equivalent diameter - WED) obtained from CT

images, and current-modulation tables provided during the topogram (scout view) to train a deep-learning algorithm to predict current-modulation for a specific scanner from images acquired at any other scanner.

The study used 50 patients (male and female, without segregation) representative of the body types range expected in our institution. Each patient underwent a thoracic CT at a GE Revolution GSI with 64 slices. The mA tables provided during the topogram for each patient were recorded. The training dataset for the deep-learning algorithm consisted of the independent variables, i.e., the WED values, and the dependent variables, i.e., the mA modulation table values.

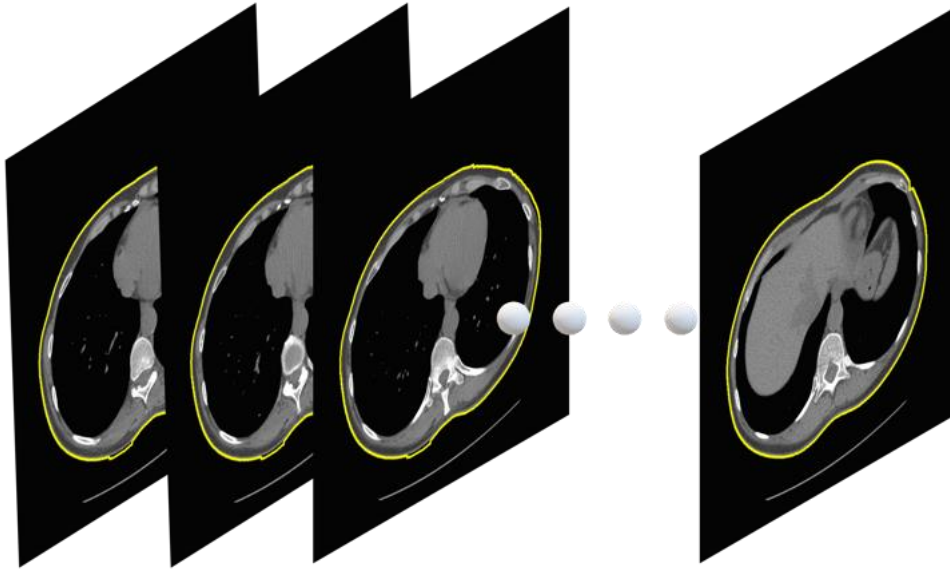


Figure 39: Example of body segmentation in various consecutive slices using morphological operations.

Each slice was processed using an automatic segmentation algorithm developed in Matlab® to determine body outlines (Figure 39). The segmentation algorithm was based on morphological image operations using a square structure element with side length equal to 12 pixels [18]. Once the outline was determined, the water equivalent diameter was estimated using the algorithm described in AAPM TG 220. The transverse position of each slice was recorded.

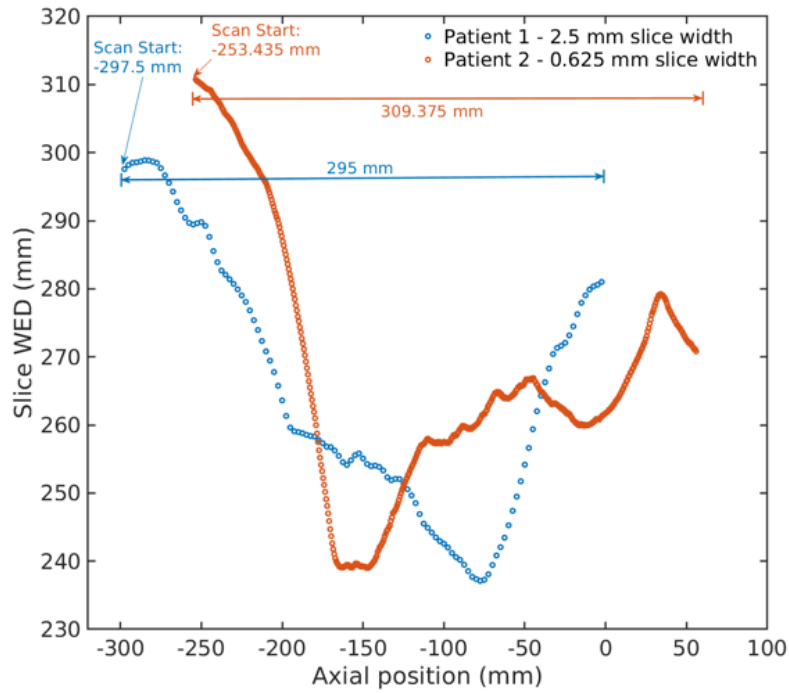


Figure 40: Differences in scan length, slice width and positioning of each patient reflect on WED values per slice.

Reconstructed slice widths and number of slices do not always match between patients. In addition, transverse slice positions are usually different for each patient and scan length has substantial variations between patients (Figure 40). These differences lead to different number and start position of WED values per patient and subsequently to an undesirable inconsistency in the independent variables of the training set. To address these challenges, the transverse position was shifted to common start for all patients, the number of WED values was linearly regressed to match same number for all patients and any missing values due to shorter scan lengths were zero-padded.

The independent and dependent values in the training and validation datasets were normalized using min-max normalization across variables (Figure 41).

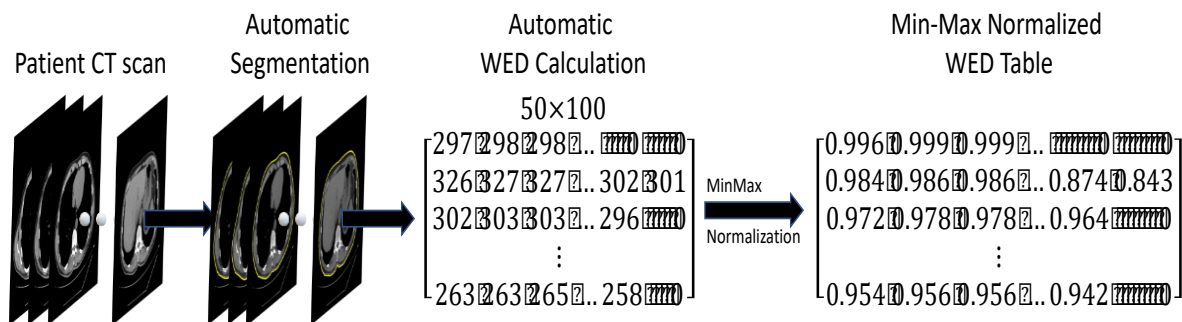


Figure 41: Procedure to determine the normalized independent variable table. (Dependent variable not shown but included in the model).

The deep-learning model consisted of a recurrent neural network (RNN) with 200 nodes, fully connected to two hidden layers with 100 and 11 nodes respectively. A 50% dropout layer was included between the two hidden layers. A 5-fold cross-validation was used (Figure 42).

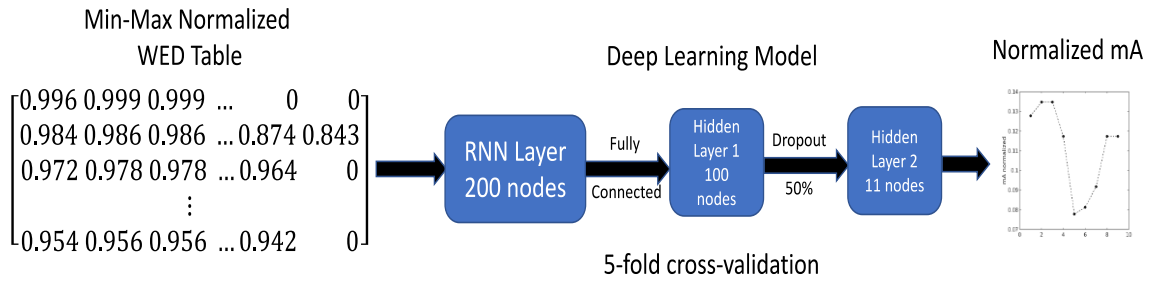


Figure 42: General structure and flow of the deep-learning model (Dependent variable not shown but included in the model).

The RNN was a long short-term memory network (LSTM) where instead of a time-series, the independent variable was considered the WED for each consecutive slice of the patient [19]. This RNN was selected based on the close relation in WED values between neighboring slices which does not necessarily reflect long term relation in WED values at the start and of the CT scan. For example, we expect similar WED values for adjacent slices in the lung but very different WED values between slices in the lung and the upper abdomen despite being part of the same CT scan of the thorax.

The training of deep-learning model was evaluated using validation loss and root mean squared error (RMSE). The RMSE and the relative difference were used to estimate the deviation of predicted mA values from tabulated mA values obtained during the CT scan.

After training, the validation loss and RMSE were  $9 \times 10^{-4}$  and 0.0436 respectively (Figure 43). The average relative difference and RMSE between predicted and actual mA values was 3.8% and 0.014 respectively (Figure 44). The predicted against the real tube-current modulation for various patients is demonstrated in Figure 45 (normalized). In Figure 46, the absolute values of predicted versus the real tube-current modulation are overlaid in a coronal slice of the corresponding patient.

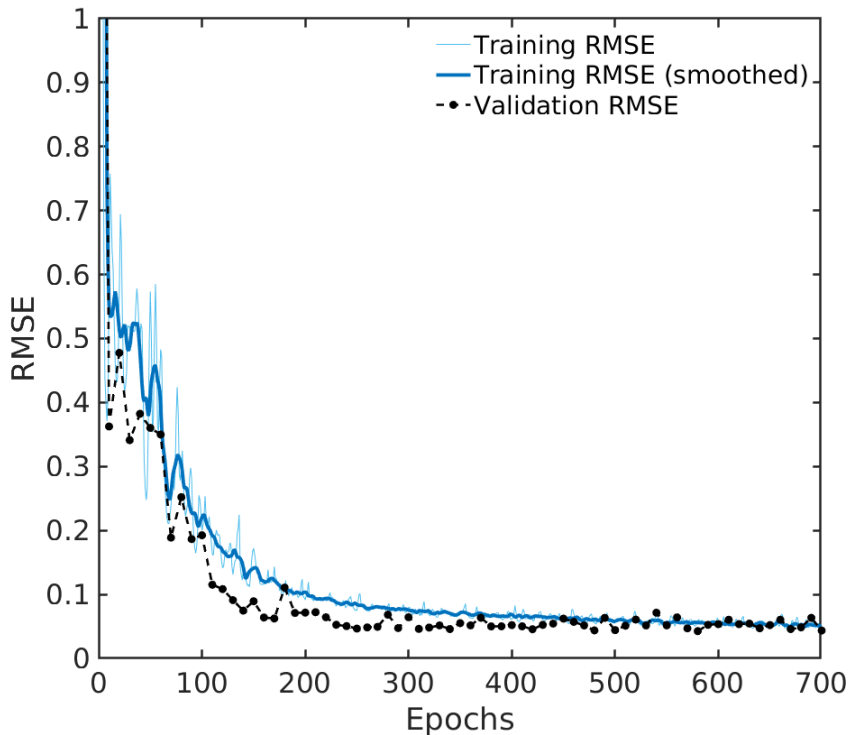


Figure 43: Validation loss and RMSE graph.

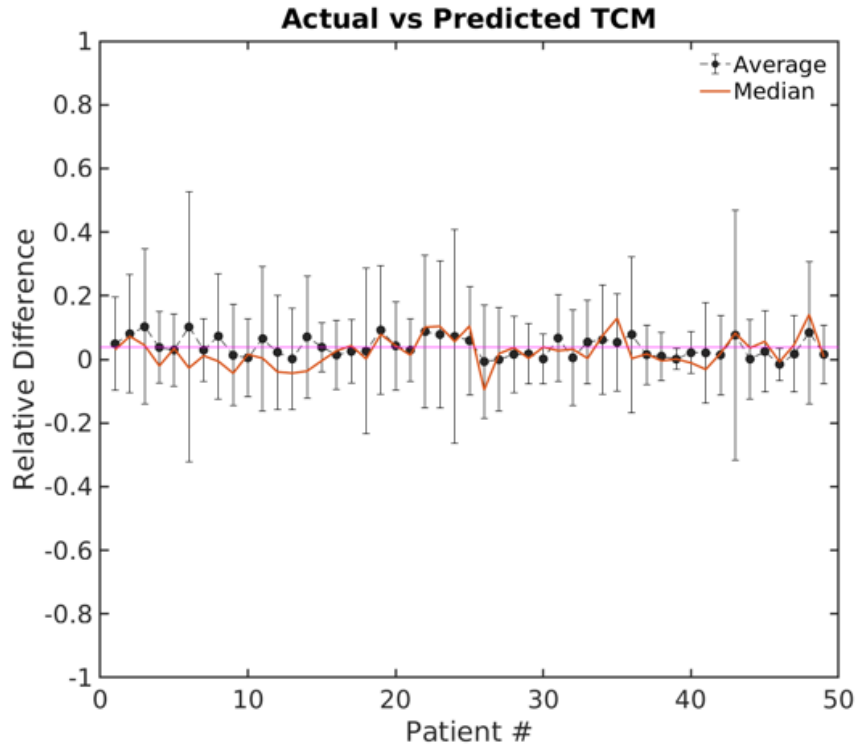


Figure 44: Relative difference between Actual and Predicted current modulation per patient.

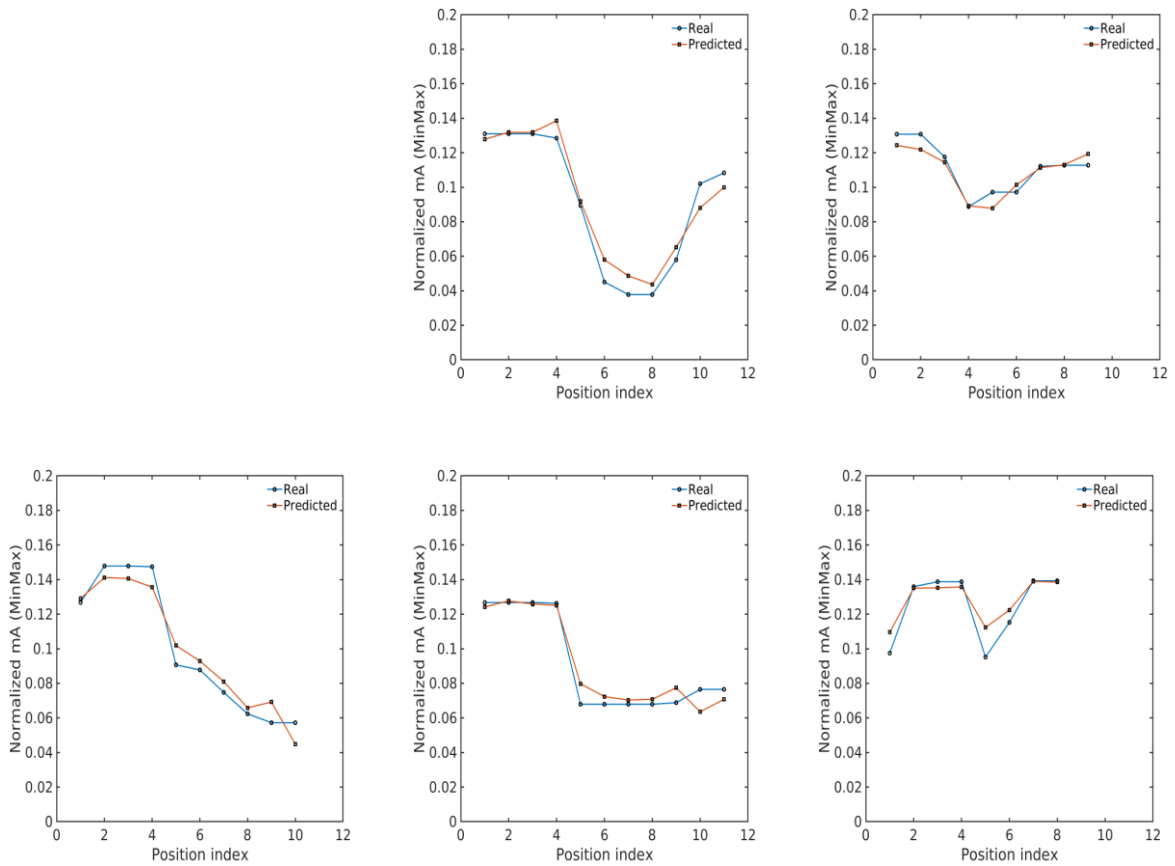


Figure 45: Predicted versus real tube-current modulation values for various patients.

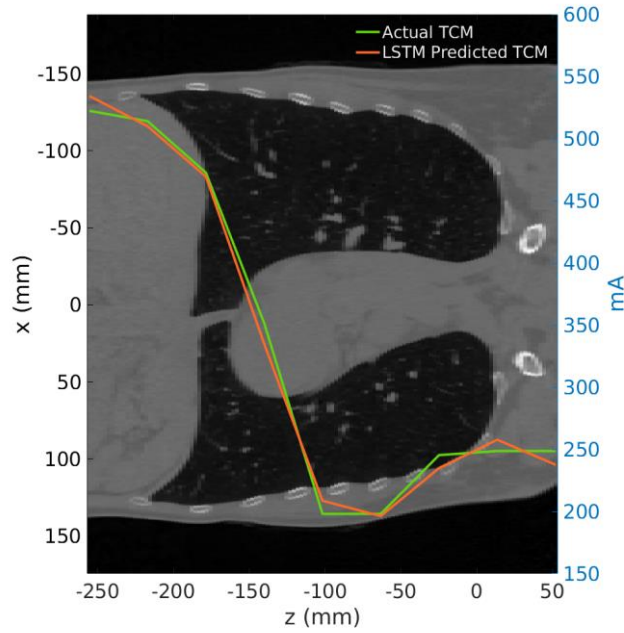


Figure 46: Predicted versus real tube-current modulation values overlaid on a coronal slice of the corresponding patient.

## 17. iDoseAI organ dose prediction module – organ dose from CT thorax scans

In this iDoseAI module, organ doses from CT thoracic scans can be predicted using the fitting parameters and dosimetric methodology explained in section 13.

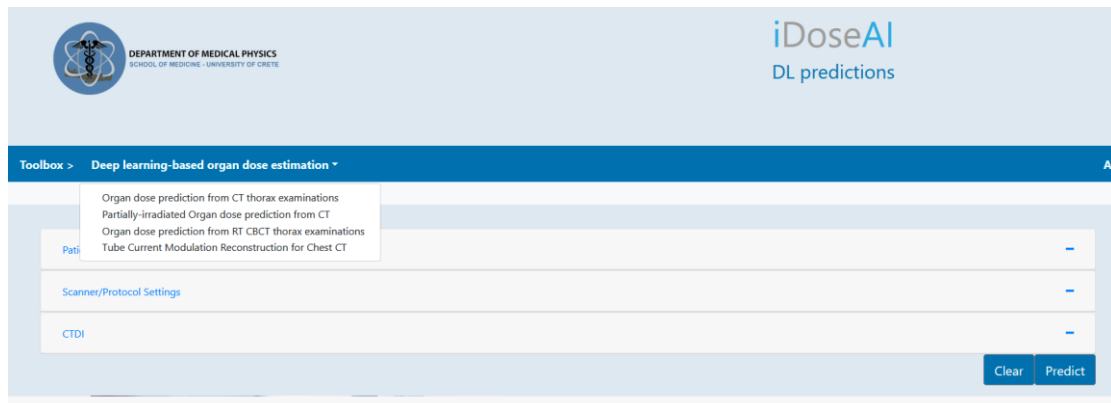


Figure 47: iDoseAI organ dose estimation tool navigation panels for of AI/ML thorax CT organ dose prediction module in accordion implementation overview.

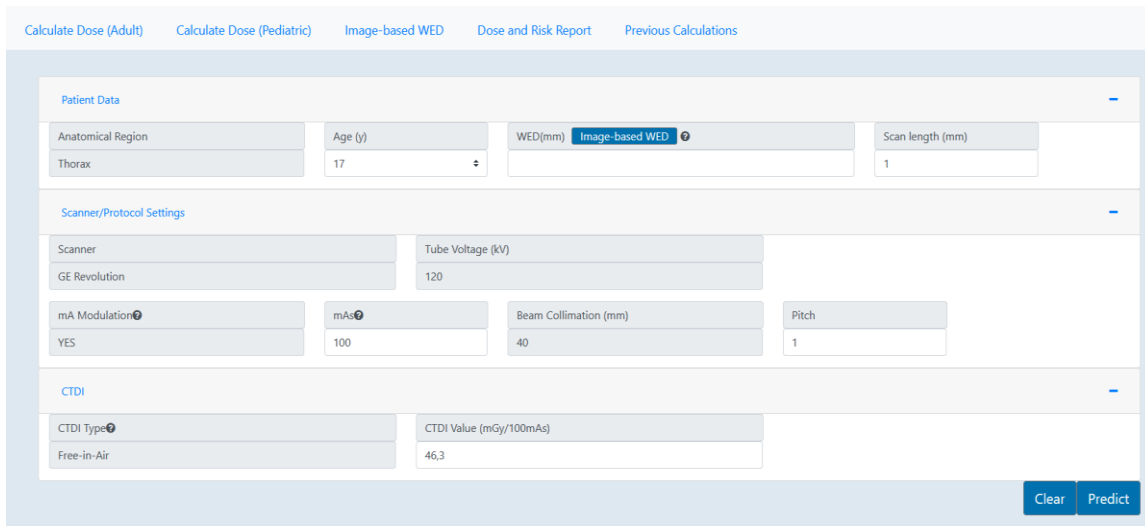


Figure 48: iDoseAI organ dose estimation tool navigation panels for of AI/ML thorax CT organ dose prediction module.

User input fields are organized into three groups:

- The ‘Patient Data’ group requires basic demographic input (i.e., age and gender), CT scan region (thorax is the only available choice for this AI module), scanning length and WED, which can either be directly inserted as a number or calculated using the automatic WED calculation tool.
- In the ‘Scanner/Protocol Settings’ group, users will select the CT scanner model (one CT model currently available) and corresponding exposure settings (i.e., kV, mA, current modulation, beam collimation, pitch, and rotation time). Users will also select the clinical indication for the CT scan.
- In the ‘CTDI Group’, users enter the CTDI type and value for their corresponding scanner.

Each group can appear or disappear on the screen as an “accordion” implementation based on the preference of the user (Figures 47, 48).

Patient Group submenu requires demographic data such as gender and age to be entered. This data is required for organ dosimetry and risk estimation. Water equivalent diameter is needed for correlation absorbed organ dose and patient size characteristics. WED is given in millimeters and can be entered as a value or calculated from user-uploaded CT data utilizing Image-based WEB tab.

Scanner Group submenu requires:

- Selection of CT scanner; Currently only one scanner is available: GE Revolution.
- Tube Voltage: Currently there is one kV selectable, 120 kV.
- mA modulation: For this AI imaging module, mA modulation is set to YES (TCM), for all calculations.
- mAs: User can manually enter the mAs of the examination. For Siemens scanners, effective mAs reading from CT console should be used.
- Beam Collimation: Beam collimation in millimeters. In MDCT the actual beam collimation is not directly correlated with slice thickness. It is the length of the individual detector (or linked detector elements) acquiring data for each of the simultaneously acquired slices that limits the width of the x-ray beam contributing to that slice, this length is often referred to as detector collimation. Beam collimation depends on CT scanner and detectors configuration. Only beam collimation of 40 mm was modeled in this module.



- Pitch: User can select pitch of the examination.
- Rotation time: User can specify time (in seconds) in which a full gantry rotation is performed.

CTDI Group submenu requires the user to enter CTDI type and value they for their corresponding scanner. CTDI values can be entered in their CTDI-free-in-air form.

## 18. iDoseAI organ dose prediction module – Partially-irradiated liver dose from CT thorax scans

In this iDoseAI module, partially-irradiated liver doses from CT thoracic scans can be predicted using the fitting parameters and dosimetric methodology explained in section 13.

Figure 49: iDoseAI organ dose estimation tool navigation panels for AI/ML partially-irradiated organ prediction module (accordion implementation overview).

Figure 50: iDoseAI organ dose estimation tool navigation panels for AI/ML partially-irradiated organ (liver) prediction module.

User input fields are organized into three groups:

- The 'Patient Data' group requires basic demographic input (i.e., age and gender), CT scan region (thorax is the only available choice for this AI module), scanning length and WED, which can either be directly inserted as a number or calculated using the automatic WED calculation tool.
- In the 'Scanner/Protocol Settings' group, users will select the CT scanner model (one CT model currently available) and corresponding exposure settings (i.e., kV, mA, current modulation, beam collimation, pitch, and rotation time). Users will also select the clinical indication for the CT scan.
- In the 'CTDI Group', users enter the CTDI type and value for their corresponding scanner.

Each group can appear or disappear on the screen as an "accordion" implementation based on the preference of the user (Figures 49, 50).

Patient Group submenu requires demographic data such as gender and age to be entered. This data is required for organ dosimetry and risk estimation. Water equivalent diameter is needed for correlation absorbed organ dose and patient size characteristics. WED and scanning are given in millimeters and can be entered as a value or calculated from user-uploaded CT data utilizing Image-based WEB tab.

Scanner Group submenu requires:

- Selection of CT scanner; Currently only one scanner is available: GE Revolution.
- Tube Voltage: Currently there is one kV selectable, 120 kV.
- mA modulation: For this AI imaging module, mA modulation is disabled (NO), for all calculations.
- mAs: User can manually enter the mAs of the examination. For Siemens scanners, effective mAs reading from CT console should be used.
- Beam Collimation: Beam collimation in millimeters. In MDCT the actual beam collimation is not directly correlated with slice thickness. It is the length of the individual detector (or linked detector elements) acquiring data for each of the simultaneously acquired slices that limits the width of the x-ray beam contributing to that slice, this length is often referred to as detector collimation. Beam collimation depends on CT scanner and detectors configuration. Only beam collimation of 40 mm was modeled in this module.
- Pitch: User can select pitch of the examination.
- Rotation time: User can specify time (in seconds) in which a full gantry rotation is performed.

CTDI Group submenu requires the user to enter CTDI type and value for their corresponding scanner. CTDI values can be entered in their CTDI-free-in-air form.

## 19. iDoseAI organ dose prediction module – Tube Current Modulation Reconstruction

A deep-learning algorithm was developed to predict normalized current-modulation for a specific scanner (GE Revolution 64) from images acquired at any other scanner and the use of size-specific metrics (such as water equivalent diameter - WED). These normalized current values can be used to simulate CT examinations through popular MC codes and applications.

For the reconstructed tube current calculation, the user is prompted with an interface to upload a single DICOM image or a DICOM series as a group of images. No images and DICOM header information are stored after exiting the Imaged-Based calculation tab, so there is no risk of sharing sensitive patient data. Tube current values, normalized to 100 mAs, per rotation are presented and the user can select/copy and use the results to simulate CT examinations (e.g. ImpactMC, EGS, Geant4 etc.).

**Toolbox > Deep learning-based organ dose estimation > Tube Current Modulation Reconstruction for Chest CT**

Patient-specific organ-dose estimation from CT examinations can be estimated with high accuracy using Monte Carlo computations. The process usually requires specific patient models, i.e., voxelized phantoms based on CT scans, and scanner-specific details (e.g., geometry, mA modulation).

A deep-learning algorithm was developed to predict normalized current-modulation for a specific scanner (GE Revolution 64) from images acquired at any other scanner and the use of size-specific metrics (such as water equivalent diameter - WED). These normalized current values can be used to simulate CT examinations through popular MC codes and applications.

Files:  Δεν επιλ... αρχεία.

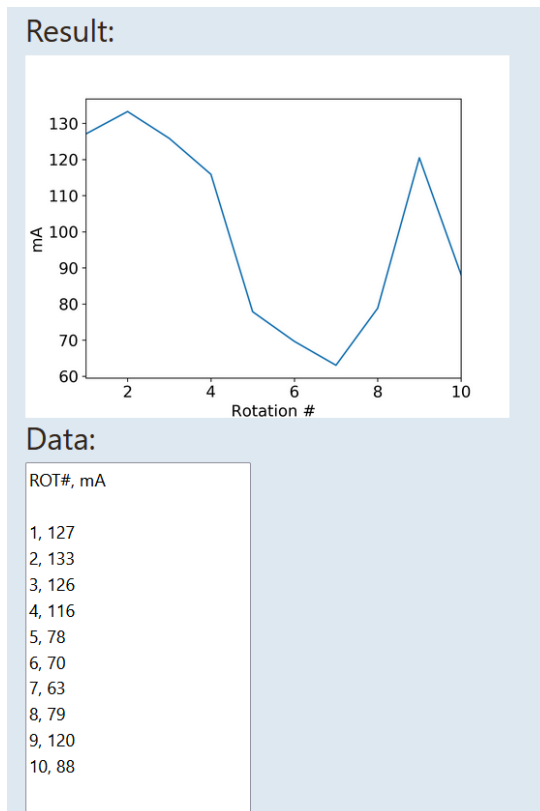


Figure 51: iDoseAI organ dose estimation tool navigation panels for of AI/ML tube current modulation reconstruction prediction module.

## 20. Dose and Risk report

Calculated organ doses from all iDose modules (X-ray imaging and AI-based predictions) can be used for the assessment of the risk of exposure-induced cancer. The risk estimates are based on the combined absolute and relative risk models of BEIR VII committee (BEIR 2006). The models consider the cancer site, sex, age at the exposure and attained age. Age-dependent mortality rates are used for subsequent assessment of lifetime cancer risk. Risk models are presented for leukaemia and solid cancers in organs that radiation absorbed dose is provided. iDose calculates the risk of exposure-induced death (cancer mortality) for leukaemia and solid cancer for those organs. Also, the user may use the risk calculation module for estimating the cancer risk (cancer incidence) resulting from a predefined single CT exposure.

Many factors, e.g., limitations in epidemiologic data for radiation-induced cancer, contribute to the uncertainty of risk estimation. The BEIR VII committee suggests that the risk estimates should be regarded with a healthy scepticism, placing more emphasis on the magnitude of the risk. The committee estimates that the excess cancer mortality due to radiation can be estimated within a factor of two (at 95% confidence level). For leukaemia the corresponding factor is four. For individual solid cancer sites, the risk estimation may have large uncertainties, up to an order of magnitude or more (BEIR 2006). BEIR VII committee assumes that solid cancers have a latency period of 5 years. For leukaemia the latency period is 2 years.

### Dose per organ (mGy)

Bone	Heart	Esophagus	Lungs	Skin	Breast
22.1	11.9	10.6	10.9	12.9	N/A

### LAR of cancer incidence

	Radiogenic (this procedure)		Other Causes
Lungs	20 in 100000	or 1 in 5097	1 in 26
Breast	N/A	N/A	N/A
Leukemia	805 in 100000	or 1 in 124	1 in 175

### LAR of cancer mortality

	Radiogenic (this procedure)		Other Causes
Lungs	3 in 100000	or 1 in 33979	1 in 31
Breast	N/A	N/A	N/A
Leukemia	537 in 100000	or 1 in 186	1 in 250

Figure 52: iDose organ dose calculation tool - Dose and risk report calculation tab.

iDose software dose and risk report tab provides a summary of the absorbed dose per organ in mGy for each primarily irradiated thorax organ, as well as values of lifetime attributable risk for exposure-induced death (LAR for Lifetime cancer mortality) and lifetime attributable risk for cancer incidence (LAR for Lifetime cancer incidence). In addition to the radiogenic risks provided for the specific CT exposures, the software provides the corresponding LARs for cancer incidence and mortality for all causes (including radiogenic) as presented for the 40 countries in the four United Nations-defined areas of Europe and for Europe and the European Union (Ferlay, 2018).

Dose and Risk Report					
<b>Patient Data</b>					
Anatomical Region	Age (y)	WED(mm) Image-based WED			
Thorax	33	280			
<b>Protocol Settings</b>					
Scanner	Tube Voltage (kV)	mA Modulation	mAs	Beam Collimation (mm)	Pitch
GE Revolution	120	YES	100	20	1
<b>CTDI</b>					
CTDI Type	CTDI Value (mGy/100mAs)				
Free-in-Air	24.2				
<b>Dose per organ (mGy)</b>					
Lungs	Heart	Bone	Bone Marrow	Esoph	Skin
8.88	9.64	13.89	5.2	7.99	8.03
<b>Lifetime Attributable Risk (LAR) of Cancer Incidence</b>					
	Radiogenic (this procedure)				
Lungs	9.30 in 100000 (0.0093%) or 1 in 10751				
Leukemia	4.39 in 100000 (0.0044%) or 1 in 22779				
<b>Lifetime Attributable Risk (LAR) of Cancer Mortality</b>					
	Radiogenic (this procedure)				
Lungs	9.30 in 100000 (0.0093%) or 1 in 10751				
Leukemia	4.39 in 100000 (0.0044%) or 1 in 22779				
<p>(*) Globoscan study 2018 for Europe attributed an overall lifetime risk of 28% for developing an invasive cancer (males: 32.1%, females: 24.7%) and an average lifetime risk of 11.9% for dying from cancer before the age of 75 years (males: 15.1%, females: 9.2%). These statistics do not take into consideration individual risk factors including lifestyle (smoking, diet, exercise, etc.), family history (genetics) or radiation exposure.</p> <p><small>Disclaimer: The aim of this report is to provide information about additional risk of cancer based on medical imaging, not to provide medical advice. Dose and risk calculations provided by the tool should be taken as estimates and may not be used solely for medical decisions. The benefits of justified medical imaging examinations almost always outweigh potential risks from ionizing radiation.</small></p>					

Figure 53: iDose Dose and Risk Report example.

## 21. References

1. Brenner DJ, Hall EJ. Computed tomography: an increasing source of radiation exposure. *N Engl J Med* 2007; 357:2277–2284.
2. Mettler FA, Bhargavan M, Faulkner K, et al. Radiologic and nuclear medicine studies in the United States and worldwide: frequency, radiation dose, and comparison with other radiation sources-1950-2007. *Radiology* 2009; 253:520–531.
3. International Commission on Radiological Protection, “The 2007 recommendations of the International Commission on Radiological Protection,” ICRP Publication 103, 2007.
4. Committee to Assess Health Risks from Exposure to Low levels of Ionizing Radiation, Nuclear and Radiation Studies Board, Division on Earth and Life Studies, National Research Council of the National Academies, Health Risks from Exposure to Low Levels of Ionizing Radiation: BEIR VII Phase 2 (The National Academy, Washington, DC, 2006).
5. The new EU General Data Protection Regulation: what the radiologist should know *Insights Imaging*. 2017 Jun; 8(3): 295–299.
6. Aryanto, K.Y.E., Oudkerk, M. & van Ooijen, P.M.A. Free DICOM de-identification tools in clinical research: functioning and safety of patient privacy. *Eur Radiol* 25, 3685–3695 (2015).
7. Schmidt, B & Kalender, WA (2002), “A fast voxel-based Monte Carlo method for scanner- and patient-specific dose calculations in computed tomography”, *Phys. Med.* 18(2): 43-53.
8. Deak, P, et al (2008), “Validation of a Monte Carlo tool for patient-specific dose simulations in multi-slice computed tomography”, *Eur. Radiol.* 18:759-772.
9. Myronakis, M, et al (2009), “Evaluation of a patient-specific Monte Carlo software for CT dosimetry”, *Rad. Prot. Dosim.*133(4): 248-255.
10. GE Revolution 64 technical manual. GE Documentation library, at <https://customer-doc.cloud.gehealthcare.com/#/cdp/dashboard>.
11. Poludniowski G et al (2009), Calculation of x-ray spectra emerging from an x-ray tube. Part II. X-ray production and filtration in x-ray targets *Phys Med Biol.* Oct 7;54(19):N433-8.
12. Tucker DM, Barnes GT, Chakraborty DP (1991), Semiempirical model for generating tungsten target x-ray spectra. *Med Phys*; 18 (2): 211–218.
13. Ridler, TW & Calvard, S (1978), "Picture thresholding using an iterative selection method", *IEEE Transactions on Systems, Man and Cybernetics* 8: 630-632.
14. Nobuyuki Otsu (1979). "A threshold selection method from gray-level histograms". *IEEE Trans. Sys. Man. Cyber.* 9 (1): 62–66.
15. MATLAB version 2021a, Natick, Massachusetts: The MathWorks Inc., 2021.
16. Keras tuner, O'Malley, Tom and Bursztein, Elie and Long, James and Chollet, Francois and Jin, Haifeng and Invernizzi, Luca and others, 2019, <https://github.com/keras-team/keras-tuner>.
17. Bergstra, J., Bengio, Y.: Random search for hyper-parameter optimization. *Journal of Machine Learning Research* 13, 281–305 (2012).

18. van den Boomgard, R, and R. van Balen, "Methods for Fast Morphological Image Transforms Using Bitmapped Images," *Computer Vision, Graphics, and Image Processing: Graphical Models and Image Processing*, Vol. 54, Number 3, pp. 252–254, May 1992.
19. Hochreiter, S., and J. Schmidhuber. "Long short-term memory." *Neural computation*. Vol. 9, Number 8, 1997, pp.1735–1780.

## 22. Appendix - Hyperparameters Optimization Algorithms parametrization

### *Random Search Algorithm – model constructor parameters*

```
kerastuner.tuners.randomsearch.RandomSearch(hypermodel, objective, max_trials, seed=None,
hyperparameters=None, tune_new_entries=True, allow_new_entries=True, **kwargs)
```

- The hypermodel parameter accepts an instance of the HyperModel class or a callable that takes hyperparameters and returns a compiled model. An example callable has been created above, which will be provided to this parameter. Alternatively, a class can be created that extends the HyperModel class and has a build() method that functions similarly to the callable mentioned earlier (taking hyperparameters and returning a compiled model). An instance of that class can then be passed to this parameter.
- The objective parameter accepts either a string value representing an Objective instance that specifies the objective function to optimize, or an instance of the Objective class itself. When a string value is provided, the Keras tuner will infer whether to minimize or maximize the objective function. For example, if 'accuracy' is given as the value, the tuner will attempt to maximize training accuracy, while 'val\_loss' will be minimized. Any string metric or loss name can be used for this parameter, such as 'val\_loss', 'loss', 'mean\_squared\_error', etc. However, when using a custom metric or loss and the tuner cannot determine whether to minimize or maximize it automatically, an instance of Objective should be provided. The Objective() constructor requires two arguments:

name: The name of the metric to monitor.

direction: A string specifying the direction of optimization, where 'min' indicates minimizing and 'max' indicates maximizing.

- The max\_trials parameter accepts an integer value that specifies the number of different hyperparameter settings to try during the optimization process.
- The seed parameter is a random seed that can be set to reproduce the same results.
- The hyperparameters parameter is optional and accepts instances of HyperParameters. It can be used to override the default settings when creating a function that builds the network. More information on its usage will be explained later.
- The optimizer parameter is optional and allows for the use of optimizers that override the one specified in the model creation method.
- The loss parameter is optional and accepts a loss function that can override the one already specified in the model creation method.
- The metrics parameter is optional and accepts a list of metrics that can override the ones already specified in the model creation method.
- The directory parameter accepts a relative path specifying where the work should be saved when the tuner explores various hyperparameter settings. By default, it is set to the current directory.
- The project\_name parameter specifies the name of the project. A folder with this name will be created, and all progress during the optimization process will be stored there. If multiple optimizations are being performed simultaneously, a different value should be provided for each tuner to ensure separate project folders. Unique names have been given to all our tuners.
- The overwrite parameter is optional and accepts a boolean value that determines whether to reload an existing project with the same name if one exists. The default value is False.



*Bayesian Optimisation Algorithm - model constructor parameters*

```
kerastuner.tuners.bayesian.BayesianOptimization(hypermodel, objective, max_trials,
num_initial_points=2, seed=None,

hyperparameters=None, tune_new_entries=True, allow_new_entries=True, **kwargs)
```

- hypermodel: Instance of HyperModel class (or callable that takes hyperparameters and returns a Model instance).
  - objective: String. Name of model metric to minimize or maximize, e.g. "val\_accuracy".
  - max\_trials: Int. Total number of trials (model configurations) to test at most. Note that the oracle may interrupt the search before max\_trial models have been tested if the search space has been exhausted.
  - num\_initial\_points: Int. The number of randomly generated samples as initial training data for Bayesian optimization.
  - alpha: Float or array-like. Value added to the diagonal of the kernel matrix during fitting.
  - beta: Float. The balancing factor of exploration and exploitation. The larger it is, the more explorative it is.
  - seed: Int. Random seed.
  - hyperparameters: HyperParameters class instance. Used to override (or register in advance) hyperparameters in the search space.
  - tune\_new\_entries: Whether hyperparameter entries that are requested by the hypermodel but that were not specified in hyperparameters should be added to the search space, or not. If not, then the default value for these parameters will be used.
  - allow\_new\_entries: Whether the hypermodel is allowed to request hyperparameter entries not listed in hyperparameters.
- \*\*kwargs:** Keyword arguments relevant to all Tuner subclasses. Please see the docstring for Tuner.

*Hyperband Optimization Algorithm - model constructor parameters*

```
kerastuner.tuners.hyperband.Hyperband(hypermodel, objective, max_epochs, factor=3,
hyperband_iterations=1, seed=None,

hyperparameters=None, tune_new_entries=True, allow_new_entries=True, **kwargs)
```

- hypermodel: Keras tuner class that allows you to create and develop models using a searchable space.
- objective: It is the loss function for the model described in the hypermodel, such as 'mse' or 'val\_loss'. It has the data type string. If the parameter is a string, the optimization direction (minimum or

maximum) will be inferred. If we have a list of objectives, we will minimize the sum of all the objectives to minimize while maximizing the total of all the objectives to maximize.

- `max_epochs`: The number of epochs required to train a single model. Setting this to a value somewhat greater than the estimated epochs to convergence for your biggest Model and using early halting during training is advised. The default value is 100.
- `factor`: Integer, the reduction factor for the number of epochs and number of models for each bracket. Defaults to 3.
- `hyperband_iterations`: The number of times the Hyperband algorithm is iterated over. Across all trials, one iteration will run about  $\text{max\_epochs} * (\text{math.log}(\text{max\_epochs}, \text{factor}) ** 2)$  cumulative epochs. Set this to the highest figure that fits within your resource budget. The default value is 1.
- `seed`: An optional integer that serves as the random seed.
- `hyperparameters`: HyperParameters instance that is optional. Can be used to override (or pre-register) search space hyperparameters.
- `tune_new_entries`: Boolean indicating whether or not hyperparameter entries required by the hypermodel but not defined in hyperparameters should be included in the search space. If this is not the case, the default values for these parameters will be utilized. True is the default value.
- `allow_new_entries`: The hypermodel is permitted to request hyperparameter entries that are not mentioned in hyperparameters. True is the default value.